POLITECNICO DI TORINO

Collegio di Ingegneria Chimica e dei Materiali

Corso di Laurea Magistrale
in Ingegneria Chimica e dei Processi Sostenibili

Tesi di Laurea Magistrale

Renal lithiasis: evaluation of the lithogenic risk through kinetics measurement of calculus growth.

Advisors

prof. Roberto Pisano
prof. Federico Mijangos Anton

Candidate

Martina Misuraca

Marzo 2021

Riassunto esteso in italiano

Introduzione

Con i termini "nefrolitiasi" o "litiasi renale" si identificano dei piccoli depositi di consistenza dura che si formano per precipitazione di sali minerali contenuti nelle urine (calcio, ossalato, fosfati ed acido urico). La formazione di un calcolo renale è favorita dall'aumento della concentrazione di questi elettroliti o dalla riduzione del liquido che li tiene in soluzione (scarso volume di urine). I calcoli renali rappresentano la terza più frequente patologia che colpisce il tratto urinario e, a prescindere da ciò, si tratta di una malattia che colpisce circa il 17% della popolazione.

A tal proposito, è bene iniziare la trattazione menzionando i reni, gli organi vitali cui si deve la formazione delle urine volta alla sua successiva espulsione attraverso il tratto urinario. I reni sono posizionati nella zona retroperitoneale, ovvero appena sopra la vita tra il peritoneo e la parte posteriore dell'addome. In un adulto normale e sano, i reni hanno una lunghezza di 10 – 14 cm, un'altezza di 6 cm e un peso di circa 150 – 170 grammi ciascuno, con il rene sinistro un po' più voluminoso di quello destro. I reni umani processano circa 190 litri di sangue ogni 24 ore ed espellono circa 2 litri di acqua e altri prodotti di scarto, che si convertono in urina. Oltre a ciò, sono anche designati per regolare le diverse proprietà del sangue, come il pH, la composizione ionica e i livelli di glucosio.

Il tasso di incidenza della nefrolitiasi, inteso come il primo evento in cui si ha la formazione della pietra, è più alto negli uomini che nelle donne, ma si registra un aumento dopo i 20 anni per gli uomini e alla fine di questi ultimi per le donne.

I fattori di rischio sono molteplici e sono tutti dipendenti dalla composizione dell'urina. Possono essere divisi in tre categorie principali. La prima è quella dei fattori di rischio non dietetici, tra cui è possibile includere la storia familiare, disturbi sistemici (tra cui obesità, ipertensione, diabete) e fattori ambientali (ad esempio, vivere in climi più caldi ed avere un'occupazione che implica l'esposizione a temperature più elevate può aumentare il rischio di sviluppo di calcoli renali). Seguono i fattori legati alla dieta, in quanto i composti maggiormente presenti nei calcoli renali sono, ad esempio: calcio, sodio, ossalati, magnesio; ciò implica che la loro assunzione influenza sicuramente la formazione delle pietre. A riguardo, è importante considerare anche la quantità di fluidi assunti, in quanto causa determinante del volume delle urine e, di conseguenza, della maggiore espulsione delle stesse. Infine, non in ordine di importanza, vi sono i fattori urinari, espressi in termini di concentrazioni, volume e pH.

Molto spesso, i calcoli renali si formano nel tratto urinario superiore e, in un minor numero di casi, direttamente nella vescica. Diversi metodi fisici permettono di identificare con precisione la natura chimica, le fasi cristalline e le proporzioni relative dei costituenti delle pietre. Generalmente sono composti da ossalato di calcio monoidrato, ossalato di calcio diidrato, fosfati di calcio, acido urico, altre sostanze organiche come urati, cistina e residui organici oppure da miscele di due o più di questi componenti. Circa l'80% di tutte le pietre contiene ossalato di calcio come componente principale, mentre gli altri composti si formano quando c'è una variazione nella composizione dell'urina o acidità (pH) dovuta a diversi motivi.

I calcoli renali possono essere classificati secondo l'origine, l'incidenza, la composizione o, ancora, in base al luogo della loro formazione: in particolare, se formati sopra la parete renale (in particolare la papilla), allora saranno indicati come pietre papillari, mentre i calcoli che si

sono sviluppati in una cavità renale saranno indicati come pietre di cavità, come mostrato in Figura 1.

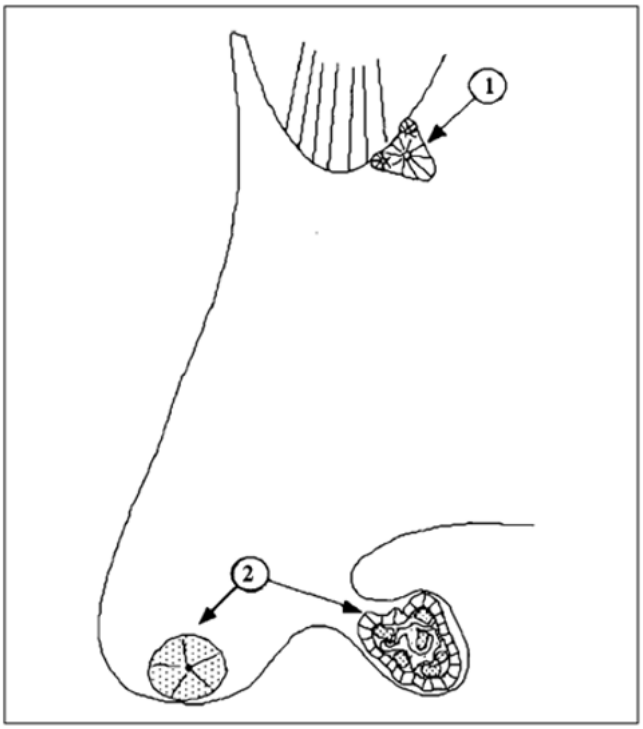

Figura 1. Rappresentazione schematica del rene e posizione di formazione di pietre ancorate - papillari - (1) e non ancorate - parte inferiore o cavità con bassa efficienza urodinamica - (2).

Il luogo di formazione della pietra suggerisce che avvenga un diverso meccanismo di formazione: mentre in quelle papillari si presume vi sia una lesione dell'uroepitelio della papilla renale, che permette la cristallizzazione e il deposito di sostanze organiche che formano un nido o il cuore di quella che sarà la guida per la crescita posteriore dei calcoli, in quelle cavitarie si suppone sia presente una cavità di bassa efficacia urodinamica, che si traduce in un maggior tempo di permanenza dell'urina nel rene, permettendo la formazione di un nido o del cuore che in seguito crescerà.

Il processo principale coinvolto nella urolitiasi è la cristallizzazione, che riguarda una transizione di fase da liquido a solido. Durante questo cambiamento, i composti disciolti in un solvente si solidificano, disponendosi secondo strutture cristalline. Da un punto di vista fisico, è quindi una trasformazione che implica una diminuzione dell'entropia.

Indipendentemente da dove avviene l'uro - cristallizzazione o indipendentemente dalla natura chimica, il requisito fondamentale per guidare la reazione è un'energia libera sufficiente, che si verifica solo quando la soluzione è supersatura. Inoltre, l'energia da superare per avviare la cristallizzazione è diversa da quella necessaria per sostenere questo processo: la prima, infatti, è maggiore della seconda.

La supersaturazione si riferisce ad una soluzione in cui la concentrazione della specie che cristallizza è maggiore della sua solubilità nella soluzione stessa e, nella maggior parte dei casi, questa è una ragione necessaria per la formazione di calcoli.

La supersaturazione diventa fondamentale: quando è bassa, il tempo necessario per la formazione di un germe cristallino è solitamente più lungo del tempo di permanenza dell'urina nel tratto urinario. Più alto è il livello di supersaturazione, più accelera la cinetica di cristallizzazione e maggiore è il numero di cristalli formati nell'unità di tempo. Parallelamente, il numero di molecole necessarie per la formazione di un germe cristallino diminuisce. In altre parole, i cristalli formati in uno stato di supersaturazione elevata sono, mediamente, più numerosi ma più piccoli di quelli osservati in condizioni di supersaturazione inferiore.

Per ciò che concerne il processo di cristallizzazione, questo è composto di differenti fasi che avvengono quasi in successione dopo il raggiungimento della condizione di sovrasaturazione; sono (in ordine): nucleazione dei cristalli, crescita dei cristalli e aggregazione dei cristalli. Questi sono mostrati in Figura 2.

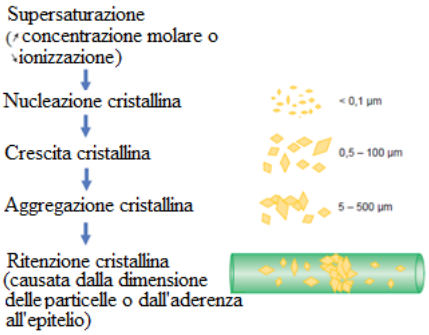

Figura 2. Fasi della cristallizzazione (tratta da Daudon, 2014, Litogénesis, *EMC Urología*, **46**: 1 – 14, con modifiche).

Il primo stadio, la nucleazione, riguarda la formazione di piccoli nuclei di cristallo. Sono formati da un numero esiguo di atomi che, però, influenzano solo per una piccola parte il volume o la massa totale del cristallo. La crescita dei cristalli è lo stadio su cui è incentrato questo lavoro: si riferisce all'incorporazione di molecole (in questo caso, ioni) dalla soluzione al reticolo cristallino ed è il principale contributore al volume o alla massa del cristallo. Senza questo passaggio, le pietre non si formeranno sicuramente. L'aggregazione si riferisce al fatto che i cristalli si uniscono e si consolidano in un corpo policristallino. Anche se questo passaggio è ciò che maggiormente consente l'aumento del volume medio delle particelle, poiché tutte le fasi della cristallizzazione avvengono quasi contemporaneamente, tutte influenzano e causano cambiamenti nei volumi e nel numero di particelle.

Il corpo umano e le sue funzioni fisiologiche primarie possono essere visti come un "edificio industriale" o, in parole migliori, come ciò che gli ingegneri chimici vedrebbero come un impianto chimico. Ciò significa che il corpo umano è studiato come un complesso assemblaggio di reattori e unità di elaborazione che scambiano massa ed energia tra loro e l'ambiente: per mantenere le loro funzioni e preservare la costanza delle condizioni interne e dell'ambiente, le trasformazioni fisico-chimiche coinvolgono la produzione e il consumo di energia. Il rilevamento, la diagnosi e la correzione delle deviazioni dal funzionamento a regime di un impianto chimico è una sfida critica, perché gli effetti di queste variazioni possono essere presenti e letali anche quando l'impianto è normalmente in funzione, e questo vale per la reazione del corpo umano a malattie e anche malattie. Sta iniziando a essere chiaro come l'analogia tra il corpo umano e un impianto chimico sia, in realtà, forte ed efficace.

Attualmente, sono tre i principali meccanismi importanti nella formazione dei calcoli nelle vie urinarie: il primo, come detto prima, è la supersaturazione o, in altre parole, la relazione tra la

concentrazione del soluto precipitante in una soluzione e la solubilità della fase minerale di formazione. Gli altri due sono i ruoli di promotori e inibitori del processo di cristallizzazione.

Tra gli inibitori della crescita del cristallo, è possibile includere magnesio, citrati, pirofosfati e zinco, che sono piccole molecole di dimensioni simili agli ioni che costituiscono i cristalli. I promotori della nucleazione dei calcoli renali sono, invece, i componenti principali dei calcoli stessi, in quanto sono le sostanze che tendono a precipitare ea formare, appunto, cristalli, se in condizione di concentrazione eccessiva. Tra queste, le più importanti sono l'ossalato, l'ammonio, il calcio e l'acido urico.

Obiettivi

In questa tesi di laurea magistrale verrà sviluppata un'indagine sulla litiasi e verrà proposto un semplice modello cinetico per la descrizione della cristallizzazione dei calcoli renali.

Attualmente, per la diagnosi e il trattamento della litiasi, vengono eseguite immagini del sangue e delle vie urinarie e/o esami analitici. Tuttavia, le concentrazioni ottenute nelle analisi corrispondono al momento della loro estrazione e ricordo e non al momento della formazione del calcolo, pertanto possono rivelarsi di scarsa utilità, soprattutto nel caso di pazienti idiopatici.

Nonostante i grandi progressi nell'indagine di questa patologia, non è nota l'esatta sequenza dei processi fisico-chimici e biologici che portano alla formazione dei calcoli urinari. La pietra è l'unica testimonianza permanente della litiasi e di tutti gli eventi che portano alla sua genesi e formazione sono impressi nella sua stessa struttura.

Per questo motivo, in questo lavoro si propone il disegno di un nuovo metodo di caratterizzazione del calcolo. Più precisamente, per analizzare i calcoli renali che sono stati estratti da operazioni chirurgiche, è stata utilizzata la Microscopia Elettronica a Scansione con Raggi X a Dispersione di Energia (tecnica SEM-EDX). È stata eseguita un'analisi morfo - costituzionale seguendo una traiettoria radiale (dalla periferia al nucleo) al fine di determinare i diversi strati che compongono la pietra e stabilire uno schema di eventi legati sia alla crescita del calcolo che al ciclo biochimico urinario. L’obiettivo finale è stabilire una scala temporale dei processi litici di crescita, al fine di poter studiare la cronologia dei diversi eventi chimici e clinici che hanno causato la patologia. Questo lavoro è stato realizzato in collaborazione con il Sanitary Investigation Institute of Biocruces (Bizkaya, Paesi Baschi) e gli Ospedali di Cruces (Bizkaya, Paesi Baschi) e Basurtu (Bizkaya, Paesi Baschi) attraverso il progetto “ALIRE”.

Materiali e metodi

Poiché l'origine e l'intera storia dei calcoli renali sono impresse nella loro stessa struttura, trovare un modo adeguato a studiarne la costituzione diventa centrale per comprendere i processi coinvolti nella sua crescita.

Di solito vengono utilizzati metodi sia chimici che fisici per analizzare la pietra ma, purtroppo, le tecniche chimiche non sono sempre sufficientemente accurate da consentire la rilevazione di alcuni elementi particolari nella pietra e la loro quantificazione in pietre miste. Inoltre, gli strumenti chimici spesso non sono in grado di specificare e differenziare le fasi cristalline dell'ossalato di calcio o del fosfato di calcio. Questo può essere importante, perché a seconda dei composti che effettivamente costituiscono la pietra, è possibile indagare e riconoscere la condizione biochimica e fisiopatologica.

In considerazione di ciò, solo i metodi fisici possono identificare tale diversità di componenti e raggiungere tali risultati e obiettivi. Diverse tecniche sono state esplorate per questo scopo, come la spettroscopia Raman (RMN), la spettroscopia a infrarossi (IR), l'analisi termica e persino la stereomicroscopia per la morfologia dei calcoli. Le limitazioni possono essere dovute ai costi e la scelta del metodo può dipendere dalla precisione e accuratezza delle apparecchiature.

Nonostante ciò, tra le tecniche utilizzate, Mijangos *et al.* (2020) hanno sfruttato la Microscopia Elettronica a Scansione con Raggi-X a Dispersione Energetica (SEM-EDX) al fine di ottenere una descrizione dei principali aspetti morfo-costituzionali di un singolo calcolo vescicale. Ciò ha permesso di considerare aspetti sia qualitativi che quantitativi della struttura della pietra (comprese le componenti minori) e di conoscere la distribuzione di questi elementi all'interno della stessa (e la corrispondente morfologia), rivelando questo tipo di approccio utile allo scopo e adeguatamente completo.

Il campione studiato è stato fornito dall'Ospedale Universitario Cruces (Barakaldo, Spagna) e si trattava di un calcolo vescicale proveniente da un paziente uomo di 74 anni, il quale soffriva di infezione urinaria ricorrente causata da *Staphylococcus aureus*. Per quanto riguarda la microanalisi della pietra, questa è stata inizialmente posta in un blocco di resina epossidica (al fine di evitarne la rottura) e poi divisa in due metà, di cui una è stata destinata all'analisi spettroscopica infrarossa mentre l'altra è stata analizzata con la SEM-EDX.

La scansione viene definita "lineare", poiché la traiettoria era radiale, dal margine esterno al nucleo della pietra. L'intensità della superficie del raggio era compresa tra 5 e 10 nA e la longitudine della traiettoria era di 2,14 mm.

Con questo specifico tipo di scansione lineare è stato possibile ottenere tutti i dati riguardanti gli elementi che costituiscono la pietra nella traiettoria studiata e adeguate informazioni sulla composizione della pietra stessa. In altre parole, conoscendo cosa è presente nella pietra, è possibile comprendere l'ambiente chimico in cui è cresciuta e gli eventi che gradualmente hanno portato alla sua espulsione.

Per perseguire un appropriato trattamento dei dati all'inizio e il raggiungimento di un modello cinetico adeguato in questo lavoro, sono stati utilizzati molti strumenti matematici e filtri. Innanzitutto, l'analisi quantitativa EDX richiede una preventiva calibrazione con campioni standardizzati ma poiché questa non potrebbe essere ottenuta per l'assenza di questi, i dati possono essere letti come le concentrazioni relative degli elementi nella pietra in funzione del radiale posizione (che è la traiettoria della scansione). Ciò può essere realizzato considerando che l'intensità di una linea di raggi X è approssimativamente proporzionale alla concentrazione di massa dell'elemento interessato.

Le concentrazioni relative ottenute sono state utilizzate per valutare il modello di crescita cinetica finale del calcolo e il valore del coefficiente di trasporto di massa.

Come accennato in precedenza, l'analisi morfo-costituzionale dei calcoli urinari ha evidenziato la presenza di bande di accrescimento e una struttura multistrato. Questi strati sono strutture ad anello di Liesegang, di cui è possibile rivelare le componenti principali in funzione dello spazio. Inoltre, ciascuna fascia di crescita corrisponde a un picco di concentrazione urinaria e un'onda di precipitazione. Nella Figura 3 sono mostrate le microfotografie della sezione trasversale della pietra. Da notare che nella figura di destra si riconosce la traiettoria seguita dalla scansione

lineare, mentre nell'immagine di sinistra si possono identificare tutti i diversi strati: ognuno di essi corrisponde alla presenza predominante di un diverso elemento, sale o composto.

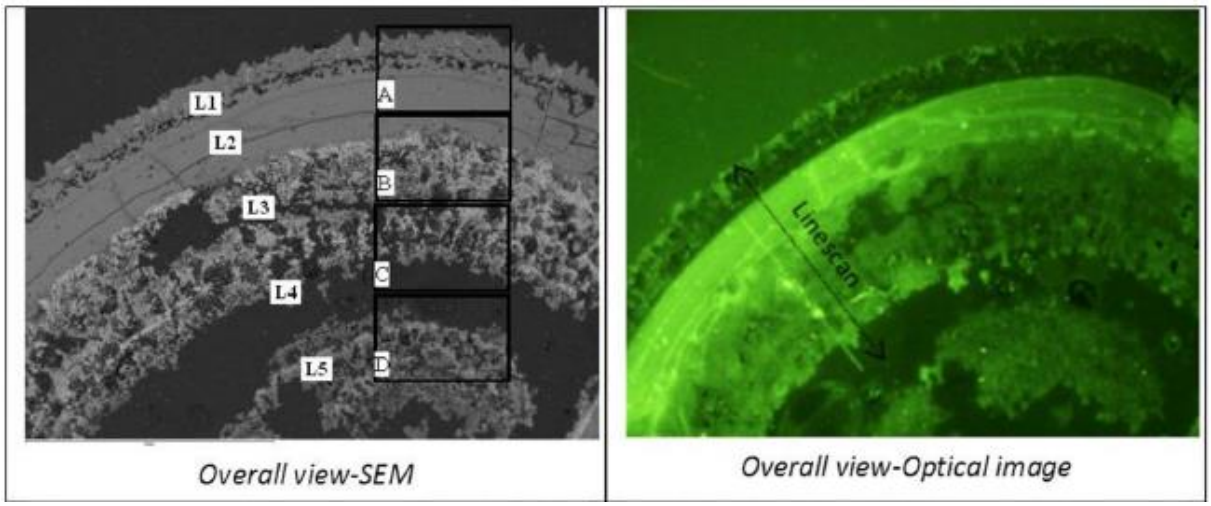

Figura 3. Microfotografie della sezione della pietra: a sinistra, la veduta d'insieme; a destra, l'immagine ottica.

Sulla base della metodologia di elaborazione dei campioni e della loro analisi, si è deciso di realizzare diverse scansioni parallele durante l'analisi SEM-EDX, con lo scopo di corroborare le informazioni ottenute sulle prime. Questa decisione è dovuta ad una morfologia variabile della superficie completa delle pietre. Solo le scansioni più rilevanti sono state prese in considerazione per l'analisi.

La prima fase di valutazione è il calcolo della massa depositata in ogni strato, considerando la posizione e lo spessore di ogni strato (che è la larghezza della banda di crescita). Per farlo, la geometria del calcolo renale è stata presa in considerazione e, più precisamente, come sferica. Inoltre, la longitudine della traiettoria lineare della scansione, pari a 2.14 mm, è stata considerata pari al raggio della pietra. Tenendo anche conto di un fattore di conversione (dalle misure rilevate dalla SEM-EDX fino ad ottenere un valore in massa) e delle percentuali delle specie cristalline nella pietra, è stato possibile ottenere i risultati per le concentrazioni mostrate nella Tabella 1.

Tabella 1. Concentrazioni (mg/cm^3) degli elementi presenti nella pietra

Elemento	Formula chimica	Valore massimo	Valore minimo	Valore medio
Carbonio	C	241	1	49
Calcio	Ca	500	5	264
Fosforo	P	133	0	35
Cloro	Cl	32	2	13
Ossigeno	O	2497	8	493
Sodio	Na	37	0	11
Magnesio	Mg	23	0	9

Potassio	K	8	1	4

Una volta scelto il calcio come elemento su cui effettuare tutti gli studi in quanto presente in maggior quantità, è possibile valutare l'andamento della sua concentrazione in funzione della posizione radiale relativa. Mentre le persone mangiano, dormono e lavorano periodicamente per ventiquattro ore, le variazioni nella composizione delle urine e nella supersaturazione tracciano le conseguenze di questo comportamento. L'escrezione urinaria dell'acqua e tutti i principali elettroliti mostrano oscillazioni circadiane, e questo tipo di periodicità è stata ben documentata nel corso degli anni e ampiamente studiata, poiché la grande maggioranza dei processi fisiologici scorre con questo ritmo. Il ritmo circadiano segna la velocità di formazione dell'urina da parte del rene ed è stato ben dimostrato che la massima escrezione avviene durante la fase di attività. Inoltre, le fluttuazioni circadiane nella cristallizzazione dei calcoli urinari suggeriscono che ci possa essere una variabilità nell'arco delle ventiquattro ore nel rischio litogenico. Applicando questi concetti alla presenza di calcio nella pietra, è stato possibile considerare ogni picco di concentrazione ad un arco di tempo pari a 24 ore e, di conseguenza, la distanza tra picchi adiacenti come un giorno. Nel caso del calcio, si sono ottenuti 21 picchi principali, per cui 21 giorni.

Nel tentativo di verificare che le onde di precipitazione ottenute mediante l'analisi SEM-EDX rispettino il ciclo biochimico dell'urina, gli studi su questo tema di Ahlstrand *et al.* (1984) sono stati presi come base di riferimento, in quanto presentano i cambiamenti nella concentrazione di vari elementi nelle urine per un totale di 24 ore, mostrando una notevole variazione nell'escrezione di questi stessi elementi, legati alle diverse abitudini di una persona durante il giorno. Mediante conversioni matematiche opportune e la rimozione del rumore relativo all'analisi SEM-EDX, è stato possibile ottenere il grafico mostrato in Figura 4, che mostra il confronto tra il ciclo circadiano del calcio durante 21 giorni per il campione studiato (arancione) e per quello di Ahlstrand *et al.* (1984; blu).

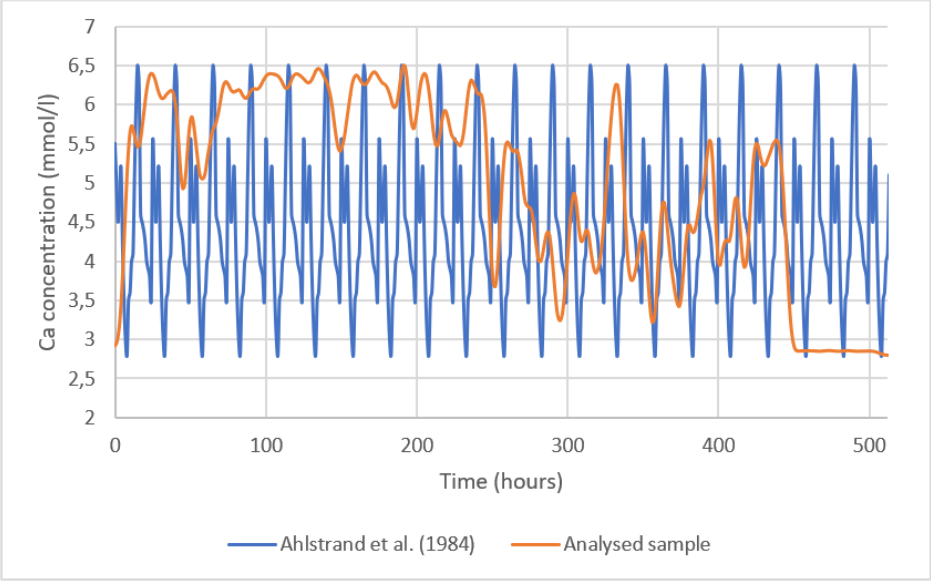

Figura 4. Confronto tra i cicli circadiani del calcio per il campione studiato (arancione) e secondo Ahlstrand *et al.* (1984; blu) in 21 giorni.

Uno sguardo più attento al grafico mostra che il profilo di concentrazione per il campione coincide anche in diversi picchi a concentrazioni inferiori. Pertanto, tenendo conto dei picchi alle concentrazioni alte e basse, nonché dei picchi con un leggero spostamento temporale, si conclude che entrambi i cicli circadiani coincidono nel 90,47%. Mentre, senza tenere conto di quei picchi con il leggero spostamento temporale, si ottiene una coincidenza del 76,2%.

Ciò conferma che i profili di concentrazione ottenuti utilizzando la tecnica innovativa proposta in questo studio possono essere correlati al ciclo biochimico delle urine in pazienti affetti da litiasi renale.

Poiché il passaggio successivo è la valutazione del livello di supersaturazione nelle urine, è importante sapere che il calcolo analitico della supersaturazione delle urine rispetto alla formazione di calcoli porta a una sorta di determinazione incompleta, poiché la composizione dell'urina è assunta senza considerare tutte le quasi 76 specie presenti in essa e, anche, considerando alcuni pH urinari fissati e non effettivi. Ciò è dovuto alla violazione della condizione di elettroneutralità, che è la legge che afferma che ogni soluzione di un elettrolita o di una miscela di elettroliti deve essere elettroneutrale (le cariche negative bilanciano le cariche positive).

Pertanto, considerando sempre il problema rispetto al calcio (più precisamente, rispetto allo ione Ca^{2+}), un pH urinario pari a 6 e la composizione di un'urina standard mostrata nella Tabella 2, è stato possibile ottenere l'andamento del livello di supersaturazione mostrato in Figura 5.

Tabella 2. Composizione di un'urina standard.

Ione/Composto	Carica	Concentrazione (mmol/L)
Na^+	1	75
K^+	1	30
Mg^{2+}	2	1.8
Ca^{2+}	2	2.5
HPO_4^{2-}	-2	5
Cl^-	-1	100
NH_4^+	1	7
Oxalate	2	0.165
Citrate	3	2.01

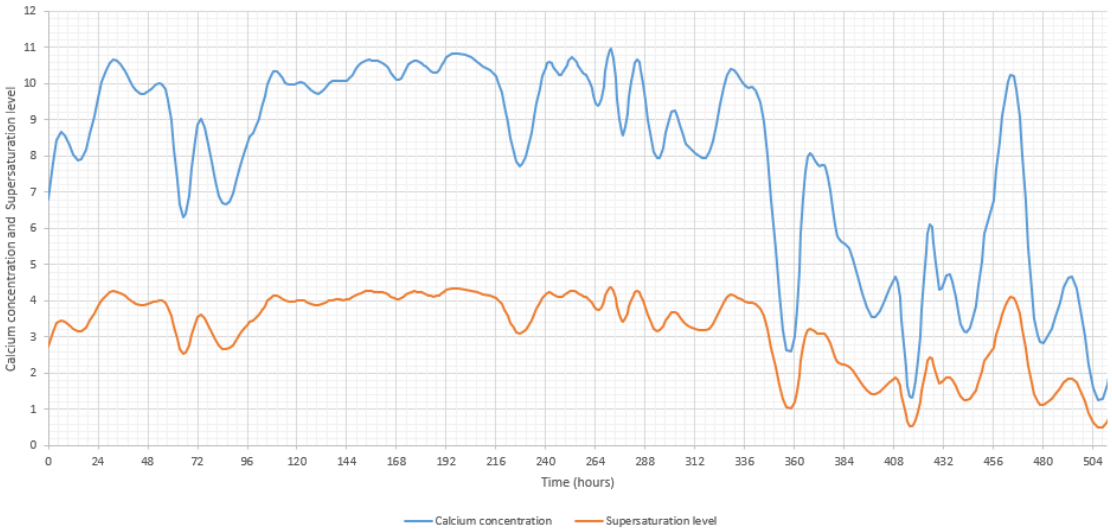

Figura 5. Livello di supersaturazione (arancione) e concentrazione del calcio (blu) nel tempo.

Si ottiene, pertanto, che la supersaturazione segue l'andamento del calcio nel tempo. Inoltre, il livello di supersaturazione è compreso in un intervallo tra 0.502 e 4.384, che corrisponde a una concentrazione di calcio nell'urina che varia tra 1.256 e 10.960 mmol/L.

A questo punto, segue la stessa comparazione eseguita per il ciclo circadiano. Secondo il modello di Ahlstrand et al. (1984), il range di supersaturazione varia tra 1.120 e 2.620. Analizzando entrambi per un arco di tempo pari a 21 giorni, si ottiene il grafico in Figura 6.

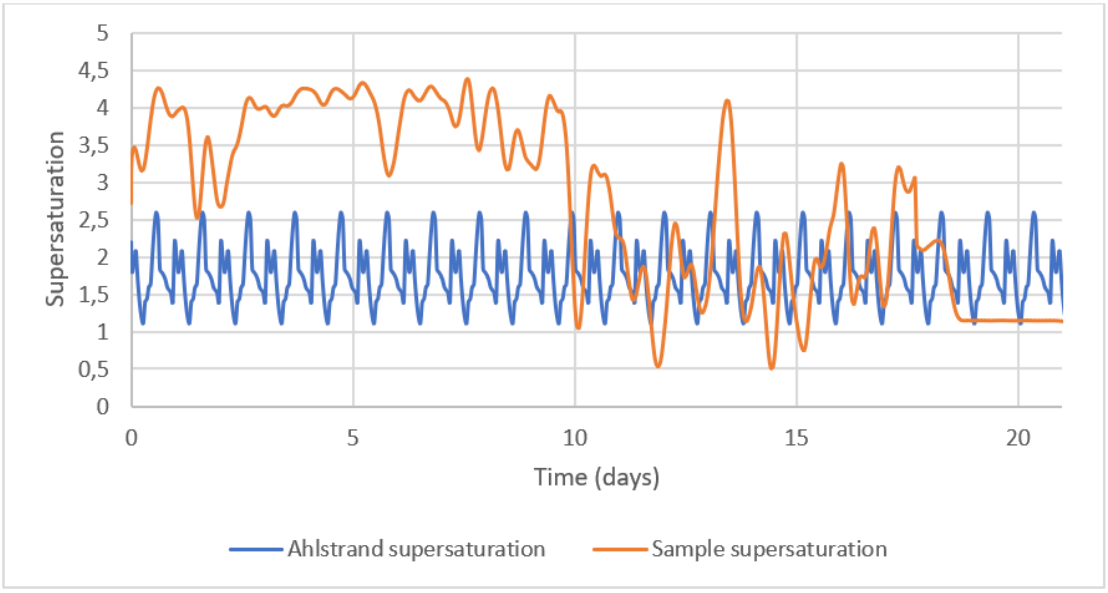

Figura 6. Supersaturazione del cacio durante un arco temporale di 21 giorni per il campione studiato (arancione) e secondo i dati di letteratura (blu).

Nonostante le notevoli differenze di valori, dovute alle differenze nelle concentrazioni di calcio considerate, l'andamento generale della sovrasaturazione è confrontabile con quello derivato dalla bibliografia considerata per questo studio.

Discussione dei risultati

È stato detto che la crescita del calcolo renale (che significa la larghezza degli strati ad anello) è considerata indipendente dalla posizione o dalla dimensione del calcolo e questo significa che la cinetica è controllata dal trasferimento di massa dalla soluzione in massa (l'urina) allo strato esterno della particella, e questo sarà descritto grazie al coefficiente di trasferimento di massa k_L. Gli effetti interfacciali e gli effetti elettrochimici non saranno considerati; quindi, queste ipotesi porteranno al modello cinetico espresso nell'Equazione 1:

$$v_g = k_L(\sigma_i - 1)S_i^* \quad (1)$$

Dove:

v_g: velocità di crescita (mm/s)

k_L: coefficiente di trasporto (mm/s)

σ_i: supersaturazione relativa della fase cristallina considerata (-)

S_i^*: supersaturazione della fase cristallina considerata (-)

Considerando, inoltre, uno stato pseudo-stazionario per la particella, è possibile concludere che la velocità di crescita delle dimensioni del calcolo renale (ovvero del raggio della particella r_p) è costante nel tempo se il livello di supersaturazione e le condizioni idrodinamiche dell'ambiente circostante la particella sono mantenute. Si ottiene, quindi, il modello cinetico espresso nell'Equazione 2:

$$\frac{d(r_p)}{dt} = \left(\frac{k_L}{\alpha_i \cdot \rho_p}\right) \cdot (\sigma_i - 1) \quad (2)$$

Dove:

t: tempo (s)

r_p: raggio della particella (mm)

k_L: coefficiente di trasporto (mm/s)

α_i: fattore di proporzionalità (-)

σ_i: supersaturazione relativa della fase cristallina considerata (-)

ρ_p: densità della particella (mg/mm^3)

Inoltre, può essere applicato anche il modello cinetico di Nernst - Planck per il flusso di ioni attraverso la superficie esterna della pietra, ma con l 'introduzione di un fattore apparente, funzione del coefficiente di trasferimento di massa e del potenziale di Nernst - Planck. Questo è mostrato nell'Equazione 3.

$$J_i a = -D_i a \frac{C_i}{RT} \Delta\mu_i \quad (3)$$

Dove:

J_i: portata molare (mol/s)

a: area specifica (mm^2/mm^3)

D_i: coefficiente di diffusione di materia (mm^2/s)

C_i: concentrazione della specie considerata (mol/mm^3)

R: costante dei gas perfetti (J/molK)

T: temperatura (K)

μ_i: potenziale chimico della specie considerata (J/mol^{-1})

Pertanto, l'Equazione 2 può essere vista come una connessione tra la prima approssimazione del flusso di tipo Fick e il flusso di tipo Nernst-Planck.

Conclusioni e prospettive future

Questo progetto di laurea magistrale mirava a un'indagine approfondita della fase di crescita di un processo di formazione del calcolo vescicale. Per raggiungere gli obiettivi di questo studio è stata fondamentale l'acquisizione preventiva di una conoscenza approfondita sull'intero sviluppo del processo litiatico; quindi, è stata condotta una profonda ricerca sulla letteratura.

Gli obiettivi più importanti raggiunti nella valutazione di un modello cinetico sono i seguenti.

- La scansione lineare SEM-EDX si è dimostrata un potente strumento per l'analisi morfo-compositiva dei calcoli urinari. Sebbene i dati grezzi di queste analisi abbiano un alto livello di rumore, questo può essere rimosso con l'applicazione di un filtro SMA per mostrare chiaramente tendenze e cicli di crescita.
- La concentrazione delle sostanze selezionate non varia in modo consistente nella fase solida, e lo stesso accade con la rispettiva solubilità.
- La sovrasaturazione locale è un fenomeno che si ripete quotidianamente e questo permette di considerare un ciclo circadiano per i parametri litogenici nelle urine e di rilevare i valori anormali.
- Piccole fluttuazioni nella composizione dei calcoli devono essere correlate alla funzione del sistema renale, poiché si è scoperto che queste sono un riflesso del ciclo biochimico delle urine. Di conseguenza, un ciclo che modifica i parametri litogenici delle urine (concentrazione di ioni che promuove l'inibizione della cristallizzazione) provoca la crescita di queste bande.
- Le fluttuazioni osservate dall'analisi SEM-EDX forniscono anche informazioni per la stima della sequenza temporale della crescita dei calcoli renali, poiché ogni picco di concentrazione può corrispondere a un giorno di formazione di calcoli.
- La crescita della pietra inizialmente oscilla ma, poi, inizia a crescere e ad aumentare: ciò può essere dovuto ad un avanzamento nel processo di cristallizzazione.
- La crescita dei calcoli è un fenomeno controllato cineticamente.
- La velocità di crescita del cristallo dipende dalla supersaturazione ma, soprattutto, dal potenziale chimico, che è il vero motore trainante dell'intero processo di crescita.

- Gli strati ad anello di Liesegang equivalgono a onde periodiche di precipitazione e picchi di concentrazione urinaria e, di conseguenza, riflettono il ciclo biologico del sistema renale.
- Il tasso di crescita della dimensione del calcolo renale (che significa il raggio della particella r_p) è costante nel tempo se vengono mantenuti il livello di sovrasaturazione e le condizioni idrodinamiche nell'ambiente particellare.
- Il tasso di crescita può essere messo in relazione con una descrizione relativa all'equazione di Nernst - Planck che descrive il flusso di ioni attraverso una membrana e considera un fattore correttivo.
- Il profilo di concentrazione del calcio segue un andamento molto simile a quello osservato nel ciclo circadiano riportato in letteratura. Pertanto, si ritiene che i pattern di concentrazione ottenuti dall'analisi SEM-EDX sul calcolo siano correlati al ciclo biochimico dell'urina.
- Utilizzando questo nuovo strumento, a differenza delle altre tecniche di analisi utilizzate finora, sarebbe possibile stabilire una sequenza cronologica di crescita del calcolo e, con queste informazioni, correlare il suo aspetto ai diversi fattori intrinseci ed estrinseci della litiasi renale e allo stile di vita del paziente.

Per quanto riguarda il processo di crescita (in senso stretto) del calcolo renale, una nuova frontiera della conoscenza in quest'area può essere lo studio dell'influenza degli effetti superficiali e delle variazioni di pressione sul flusso di ioni attraverso la superficie del calcolo. Questo tipo di approccio permetterebbe quindi di ampliare la conoscenza sulla natura delle cause della formazione e, di conseguenza, si spera di aiutare a prevenire o curare questa malattia così comune.

Index

1. Introduction

1.1 Historical background

The common terms kidney stones, nephrolithiasis or urolithiasis refers to the presence of stones within the urinary tract. This condition is known as Urinary Stone Disease (USD) (Corbo *et al.*, 2006).

More precisely, urinary stones represent the third most frequent affliction of the urinary tract, preceded by urinary tract infections and pathologic prostate illness (Stoller *et al.*, 1995) and, apart from that, an affliction that influence about the 17% of any given population (Moran, 2014).

In every aspect, but most of all in medical ones, knowing the past and how something has been studied and looked at allows generalists and specialists alike to explore a topic from an extraordinary perspective, which is the history's one. This exact method permits to obtain a new perspective, putting together knowledge and events and creating a new pathway to follow in order to obtain always more development towards the predetermined goal.

Despite this approach, attaining this kind of information and data for a medical disease, kidney stone in particular, is quite a challenge. What is known about this topic starts from the medical writing of ancient Greek, Roman, and Far and Middle East (Jones, 1924).

After the Dark Ages, that saw the fall of this kind of study, the Renaissance saw, instead, a new birth of interest and approach. From a scholarly point of view, the reawakening of medical science of the humanistic period was the real trigger of investigations, which started with the rise of anatomists Andreas Vesalius and William Harvey (Moran, 2010).

It is possible to show a timeline for the most important urolithiasis studies (BCE = before current era, CE = current era) (Prein, 1963).

About this, one of the most important discoveries that deserves to be mentioned is the one ascribable to Alexander Randall (1818 – 1872): professor of urology at the University of Pennsylvania, in 1937 he published the paper that first described the plaque named in his honour. After a number of 429 pairs of kidneys, he showed that around the 17% presented papillary lesions. These lesions were located inside the urothelial covering, near the tip of the papilla and were cream coloured. With a microscope it seemed a plaque of calcium in the interstitial tissue, definitely not inside the tubules. He saw that it arose in the basement membranes of the terminal tubule walls and involved the space between the tubules as it grew larger (interstitial means in between the tubules and vessels).

After a number of cases, he found a tiny black stone growing right on the plaque where the lining epithelium had given way, so urine could bathe the tissue deposits. It can be shown in Figure 1.1. The tiny reddish black round dot is in the middle of a white or cream coloured clearing on the papilla.

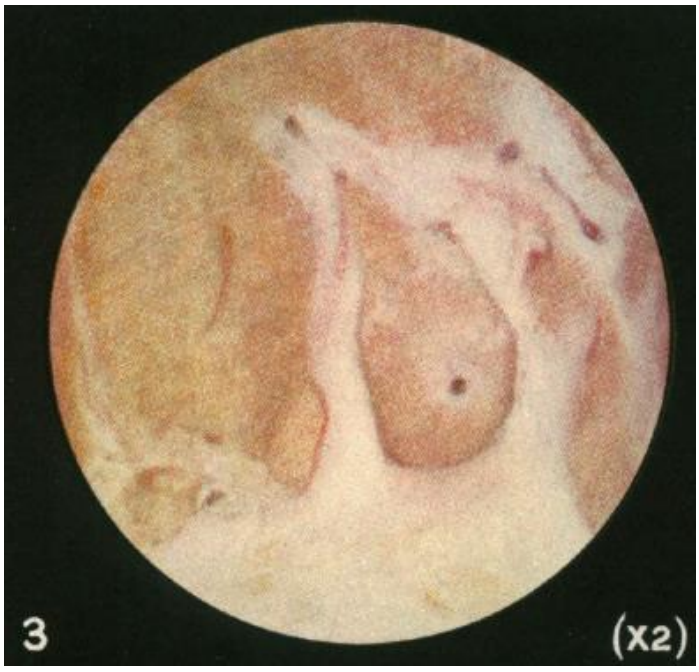

Figure 1.1. First photograph of Plaque with Stone.

Instead, by looking at the first micrograph of the following thin sections of the stone that he has been able to perform, shown in Figure 1.2, it is possible to see the stone itself and the underlying plaque. More precisely, in the image there is the tissue from the place from the place where the stone grew over plaque and the stain colours calcium. The papilla has lost its covering epithelium. The rings of colour are around tubules whose lumens remain open. In other words, the calcium deposits in the collagen that supports the tubule lining cells but does not break through into the tubule to form plugs.

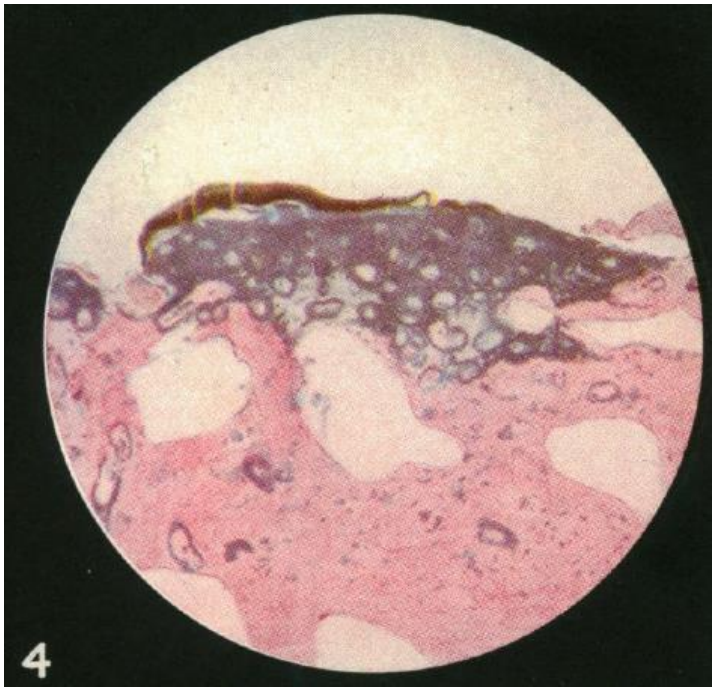

Figure 1.2. First Micrograph of plaque with stone over it.

The following list is the mentioned timeline, as reconstructed by Moran (2014):

- 1st known stone formed (5500 BCE, female bladder stone, Mesolithic)
- 1st known kidney stone (circa 3300 BCE)
- Hippocrates (460–370 BCE)
- Aristotle (384–322 BCE)
- Epicurus (341–270 BCE) suffered from kidney stones and colic
- Aulus Cornelius Celsus (25–50 CE)
- Galen (131–201 CE)
- Paul of Aegina (625–690 CE)
- Indian Vedas (Sushruta 400 CE)
- al-Razi (Rhazes 890–923 CE), (Avicenna 980–1036 CE), al-Zahrawi (Albucasis 1050–1106 CE)
- Henri de Mondeville (c1260–1316)
- Guy de Chauliac (c1300–1368)
- Philippus Aureolus Theophrastus Bombastus von Hohenheim (Paracelsus 1490–1541)
- Pierre Franco (1500–1561)
- Felix Würtz (c1500–1590)
- Battista da Rapallo and Mariano Santo da Barletta (De LapideRenum 1535) (1488–1577)
- Lanfranc (Pierre Franco 1500–1561)
- Ambroise Pare (c1510–1590)
- Andreas Vesalius (1514–1564)
- William Harvey (1578–1657)
- Frere Jean de Beaulieu (Jacques 1651–1714–1719), Claude-Nicolas Le Cat, Jean Baseilhac (Frere Come 1703–1781)
- Johann van Beverwijck (1594–1647)
- Thomas Sydenham (1624–1689) & Herman Boerhaave (1668–1738)
- Rev. Stephen Hales (1677–1761)
- William Cheselden (1688–1752) fastest lithotomy at 54 s (mortality 17 %)
- Robert Whytt (1714–1767)
- Joanna Stephens (c1739) stone formula
- John Hunter (1728–1793)
- Erasmus Darwin (1731–1802)
- Carl Wilhelm Scheele (1742–1786)

- George Pearson (1751–1828)
- William Hyde Wollaston (1766–1826)
- Alexander Marcet (1770–1822)
- English school [George Owen Rees (1813–1889), Henry Bence Jones (1813–1873), John Howship, William Henry (1774–1836), William Prout (1785–1850), Golding Bird (1814–1854), Richard Bright (1789-1858)], French school [Felix D'Azyr (1748–1794) Antoine F. Fourcroy (1755–1809), Nicolas L. Vauquelin (1763–1829), Gay-Lussac (1778–1850), F. Magendie (1783–1855)]
- Jean Civiale(1792–1867) (January 13, 1824—lithotrity) Necker Hospital in Paris
- John Yelloly (1774–1842)
- Sir Henry Thompson (Victorian urologist 1820–1903)
- Alex Copland Hutchison (1830)
- Henry Vandyke Carter (1831–1897)
- St. Peter's Hospital for Stone (1860)
- Henry Bigelow (1818–1870) Litholapaxy
- J. Swift Joly (1876–1944)
- Eugene F. DuBois (1926) parathyroid disease and stones (Captain Charles Martell) (1882–1959)
- Alexander Randall (1883–1951)
- Fuller Albright (1900–1969)
- William H. Boyce (1918–2012)
- Birdwell Finlayson (1932–1988)
- Martin Resnik, Joseph Segura, Steven Streem, Lynwood Smith, Bill Robertson
- Fred Coe, Charles YC Pak, Rosemary Ryall, Saeed Kahn, George Drach, Neil Mandel
- Ralph Clayman, Arthur Smith, Glenn Preminger, Christian Chaussy, James Lingeman, Marshall Stoller, Hans Tselius, John Asplin, Andrew Evan, Dean Assimos, Margaret Pearle, John Lieske, etc.

Thinking about the modern age, a lot of evolution is due to clinical chemistry investigation advent and, most importantly, to the use of new technologies to investigate the composition of kidney stone in order to consent a better diagnosis and the research of the pathophysiology and the physical-chemical aspects of the multiple types of urolithiasis. Among them, radiology, X-Rays, Infrared Spectroscopy.

Despite the great progress the study of renal lithiasis has seen, the origins of its etiopathogenesis continue to be unknown. In other words, the sequence of events from the genesis of calculus to its formation has not yet been fully described and known.

In this sense, the analysis of the calculation, intended as the only permanent witness of lithiasis, could be an advance in the study of its etiopathogenesis, since in its structure there are already all the events that occurred and/or the description of the physical and chemical environment present during his training.

1.2 The kidney and its functions

The basic function carried out by the kidneys is the formation of the urine for its later elimination through the urinary tract (*National Kidney and Urologic Diseases Information Clearinghouse*, 2009).

These vital organs found themselves positioned in the retro-peritoneal zone (Restrepo, 2007), which means just above the waist between the peritoneum and the back of the abdomen (Killeen, 2017). In a normal and healthy adult, the kidneys have a length of 10-14 cm, a height of 6 cm and a weight of around 150-170 grams each, with the left kidney a little more voluminous of the right one (Restrepo, 2007).

In Figure 1.3, it is shown the anatomy of the male and female urinary system, in which the position of the kidneys is observed.

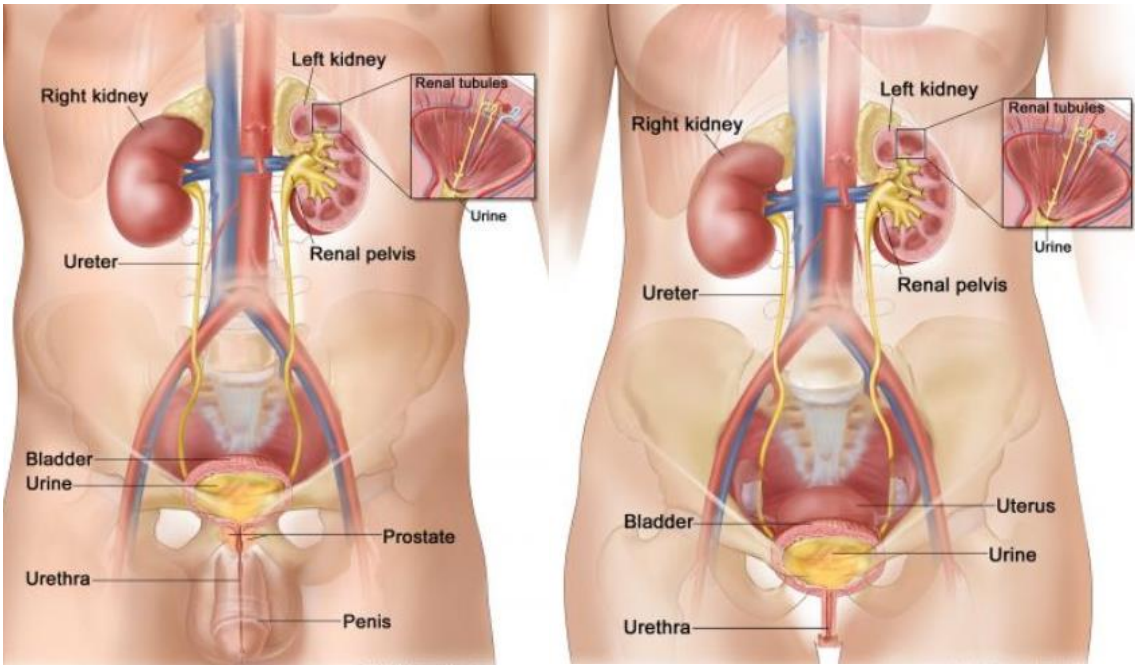

Figure 1.3. On the left side, anatomy of the male urine system. On the right side, anatomy of the female urine system (adapted from Winslow, 2010).

Human kidneys process approximately 190 litres of blood every 24 hours and expel roughly 2 litres of water and other waste products, that convert themselves into urine (NKUDIC, 2009; Rodríguez Fernández, 2013).

Filtration of blood in the kidneys occurs in the nephron, where the glomerulus acts as a filter, letting the plasma pass inside while keeping cells and proteins in the bloodstream (Killeen, 2017; NKUDIC, 2009).

In Figure 1.4, a recurring scheme of path that carries blood through the kidney and the subsequent exit of urine to the bladder is shown.

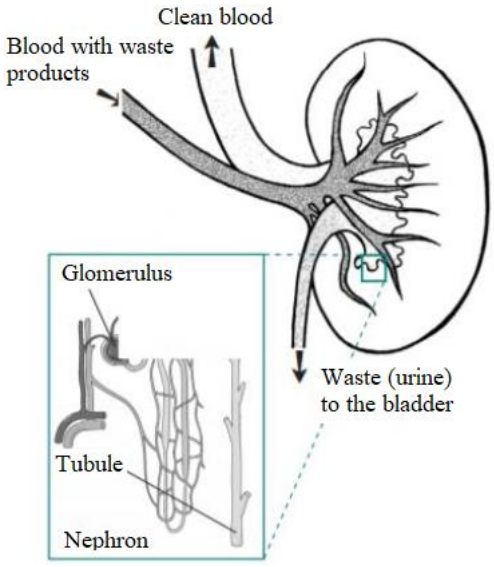

Figure 1.4. Scheme of the blood filtration by the kidney and of the expelling of urine by the urinary tract to the bladder.

Other than the excretion of discards and other substances in the urine and the production of hormones, the kidneys are also designated to regulate the proprieties of the blood, like pH, ionic composition, glucose levels and so on (Killeen, 2017).

1.3 Epidemiology

Only in the United States, this disease counts from 7 to 12 cases every 10000 people per year (Foster *et al*., 2009), but in the recent decades these numbers increased steadily given the fact that the risk factors depend on a very large spectrum of aspects, from diet to environment (Scales *et al.*, 2012). Another explanation may be due to the technological developments in the radiologic equipments and instruments used to detect the disease.

This awareness, combined with the great number of people visiting hospitals and emergency departments because of the problems deriving from this illness (Foster et al., 2009), makes relevant the investigation on this subject, in order to help finally find a way to prevent and make more easily curable this pathology.

Furthermore, research in this area, especially from an engineering point of view, can prove to be a useful and effective tool for achieving the objectives previously mentioned. What this work aspires to, together with previous and certainly future ones, is to offer a new approach to the problem.

Nephrolithiasis' prevalence varies with sex, geography, race and, mostly, with age. It has been studied that the lifetime risk of kidney stone formation is higher in men than in women: we can observe, in fact, a 12% against a 6% (Johnson *et al.*, 1979). Despite this, new data and studies from the Nationwide Inpatient Survey found a new male to female ratio of 1.3:1, substantially lower than the previous one (Scales *et al.*, 2007).

The incidence rate of nephrolithiasis, interpreted as the first stone event, is higher in males than females. The rise starts after age 20 for men and in the late twenties for women (Curhan *et*

al., 1997). Again, more recent studies show that the rates have levelled off in women and have fallen in men (Lieske *et al.*, 2006).

In addition, recurrence rates can also be considered as reliable: studies show that 30-40% of untreated individuals will form another stone in a temporal arch of 5 years after the initial one (Johnson *et al.*, 1979). As before, this formation will depend on the great variety of factors shown later in this work and, in any case, specific interventions may reduce the recurrence of the 50% or even more (Borghi *et al.*, 2002).

1.4 Risk factors

Risk factors are all affected by the urine composition. They may be divided into three main categories: non-dietary, dietary and urinary.

1.4.1 Non-dietary factors

In this case, it is possible to include family history, race, systemic disorders and environmental factors.

It has been shown that common forms of stone disease are heritable, which means that the risk is higher for people with individuals of their families that suffered from this illness (Goldfarb *et al.*, 2005). Despite this, genetic causes are still not been studied enough to be proved.

Mente *et al.* (1997) proved that people with Arabic, Indian, Latin American and Asian descent have a higher risk of stone formation in relation to people with European origins.

For what concerns systemic disorders, the pathology studied is part of them and is influenced by other ones. An example may be obesity: it has been proved that people with higher body mass index (BMI) are more likely to suffer from this illness, as urinary composition depends on it. More specifically, higher BMI is associated with greater level of urin oxalate and lower urin pH, which means that calcium oxalate or uric acid stones are more likely to form (Taylor, 2006).

Other examples of systemic disorders that may cause the suffering from kidney stone disease and the increasing of the risk of this pathology are: Chron disease, hypertension, diabetes, hyperthyroidism.

Likewise, difficulty of provides for water supplies and bathroom facilities may lead to lower fluid intake and lower urine volume.

Another aspect that needs to be taken into account is the environmental condition: it has been conjectured that living in warmer climates and having an occupation that involves the exposure at higher temperature may be increasing the risk of the development of kidney stones.

An explanation of this phenomenon may be seen in the combination of several different causes, like increased water loss due to heat, higher exposure to vitamin D, low fluid intake.

These factors can be a problem as they lead to lower urine volume and consequential changing of its composition (Corbo and Wang, 2019).

1.4.2 Dietary factors

Diet is surely one of the most important factors to be considered when approaching to the study of kidney stones: German philosopher Feuerbach, in 1804, believed that "we are what we eat"; in a certain way, transcending from the consciousness – physical relationship implied by the philosophical thesis, it is possible to apply this concept at the onset of nephrolithiasis, as dietary intake modifies and influences urine composition.

Calcium, oxalate, sodium, animal protein, sodium, magnesium and potassium are the most decisive compound related to kidney stone. The most important ones are the first two.

Studies have shown that, contrary to what one may think, higher calcium intake causes a lower risk of incident nephrolithiasis, in an independent way respect to other risk factors (Curhan G. *et al.*, 1997): dietary oxalate absorption and urinary oxalate excretion are increased if there is a lower calcium intake.

Instead, dietary oxalate absorbed by the human organism ranges from 10% to 50% and this means that a high oxalate diet may lead to the formation of renal calculi. It is not still very clear what causes the absorption, but some possible causes may be dietary factors and intestinal flora, other than medical conditions that cause the malabsorption of the oxalate (Holmes *et al.*, 2004).

Another aspect that needs to be mentioned is fluid intake, as it is the main determinant of urine volume and, consequently, of stone formation: a consistent fluid intake cause a higher output of urine and, if this latter is more than 1 L/day, risk of stone formation drops drastically (Curnhan *et al.*, 1993).

1.4.3 Urinary factors

Analysis of 24-hours urine is surely the cornerstone to know how human metabolism is currently working and makes it easier to provide information, guidelines and recommendations over what to potentially change or prognostic data.

It is significant to convey that stone formation is not a problem of amount of outtake but of concentration. In these terms, hypercalciuria, hyperoxaluria and hypocitraturia needs to be specified.

If the urine calcium excreted is more than 300mg/day (7.5 mmol/day) for men or it is more than 250 mg/day (6.25 mmol/day) for women, it is possible to talk about hypercalciuria and this is something that great part of patients who suffer from kidney stone disease experience (Curhan and Taylor, 2008).

The same goes for hyperoxaluria and hypocitraturia: the first one refers to a urine oxalate excretion greater than 45 mg/day (0.5 mmol/day), while the second points out to an amount less than 320 mg/day (1.67 mmol/day) in a 24-h urine sample. Coe (1978) has shown that an increase of urinary citrate from the normal or high range leads to an additional protection over the studied pathology.

These just presented conditions cause the variation of the urine composition, in terms of concentrations, volume and pH. More specifically, they increase the concentrations of the correspondent ions and there is a high probability of formation of stones when the condition of supersaturation in urine is reached. Moreover, they lead to the formation of a stone composed mainly by calcium oxalate and calcium phosphate, that is the more frequent type of ureteral stone encountered in patients that suffer from this illness (Brener *et al.*, 2011).

All the above-mentioned risk factors are summed in Figure 1.5.

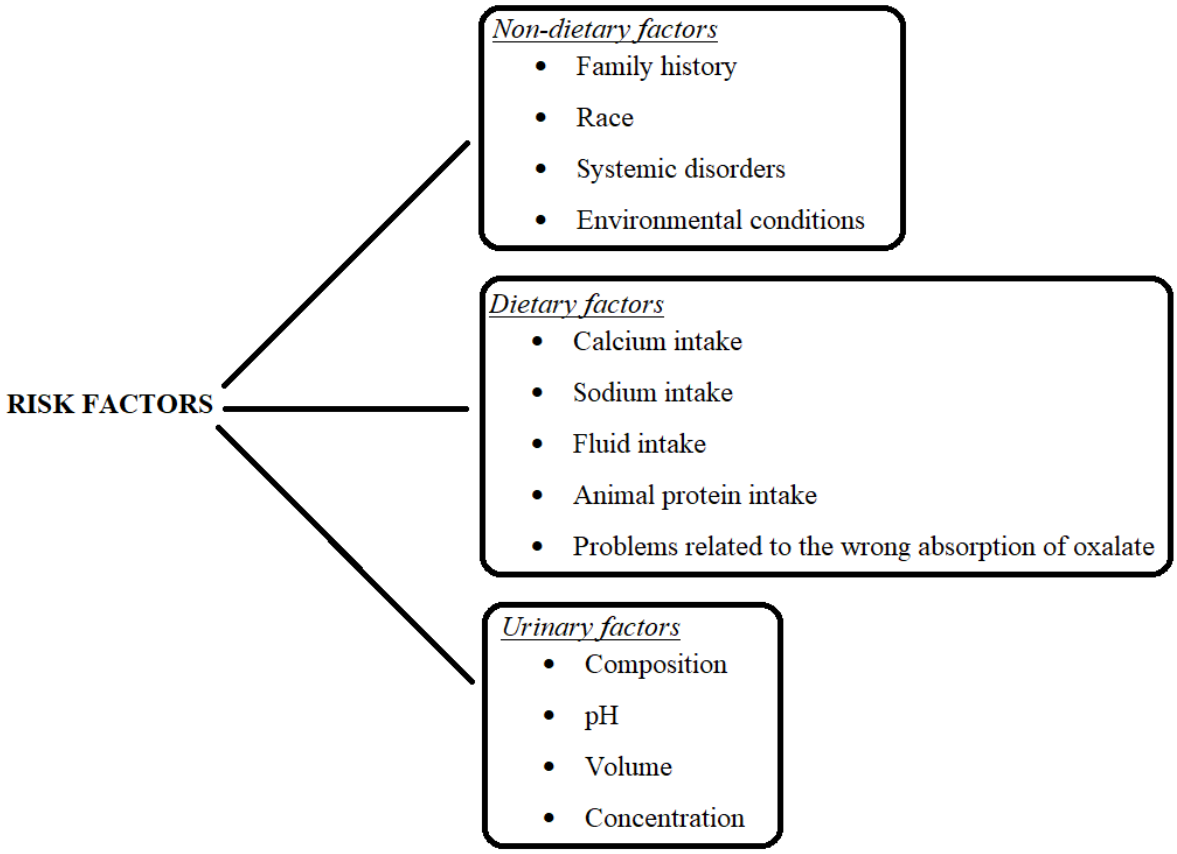

Figure 1.5. Summation of the main risk factors connected to kidney stone disease.

1.5 Types of kidney stones

Kidney stones are little aggregation of mineral salts that form in the upper urinary tract (just in a few cases they form directly in the bladder). Their presence is often related to an incongruous diet which is necessarily associated with an underlying genetic predisposition.

Physical methods allow to accurately identify the chemical nature, crystalline phases and relative proportions of stone constituents. Generally, they are composed of calcium oxalate monohydrate, calcium oxalate dihydrate, calcium phosphates, uric acid, other organic substances such as urates, cystine and organic residues or by mixture of two or more of these components (Daudon, 2016).

About the 80% of all the stones contain calcium oxalate as main component, while the other compounds form when there is a variation in the urine composition or acidity (pH) due to different reasons. In order to simplify this work, it is possible to introduce the main compounds annotated previously, as it can been seen in the table 1.1.

Table 1.1. Main compounds of kidney stones.

IUPAC Name	Acronym	Chemical formula
Calcium oxalate monohydrate	COM	$CaC_2O_4 \cdot H_2O$
Calcium oxalate dihydrate	COD	$CaC_2O_4 \cdot 2H_2O$
Calcium hydrogen phosphate dihydrate	BRS	$CaHPO_4 \cdot 2HO$
Magnesium ammonium phosphate hexahydrate	SV	$MgNH_4PO_4 \cdot 2H_2O$
Hydroxyapatite of Ca^{2+}	HAP	$Ca_{10}(PO_4)_6(OH)_2$
Carbonated hydroxyapatite	CAP	$Ca_5(PO_4CO_3)_3OH$
Anhydrous uric acid	UAA	$C_5H_4N_4O_3$
Uric acid dihydrate	UAD	$C_5H_4N_4O_3 \cdot 2H_2O$

Mineral forms of COM, COD, BRS and SV are, respectively: whewellite, weddellite, brushite and struvite. Their shape and how they look like depends on their composition: few examples are shown in Figure 1.6.

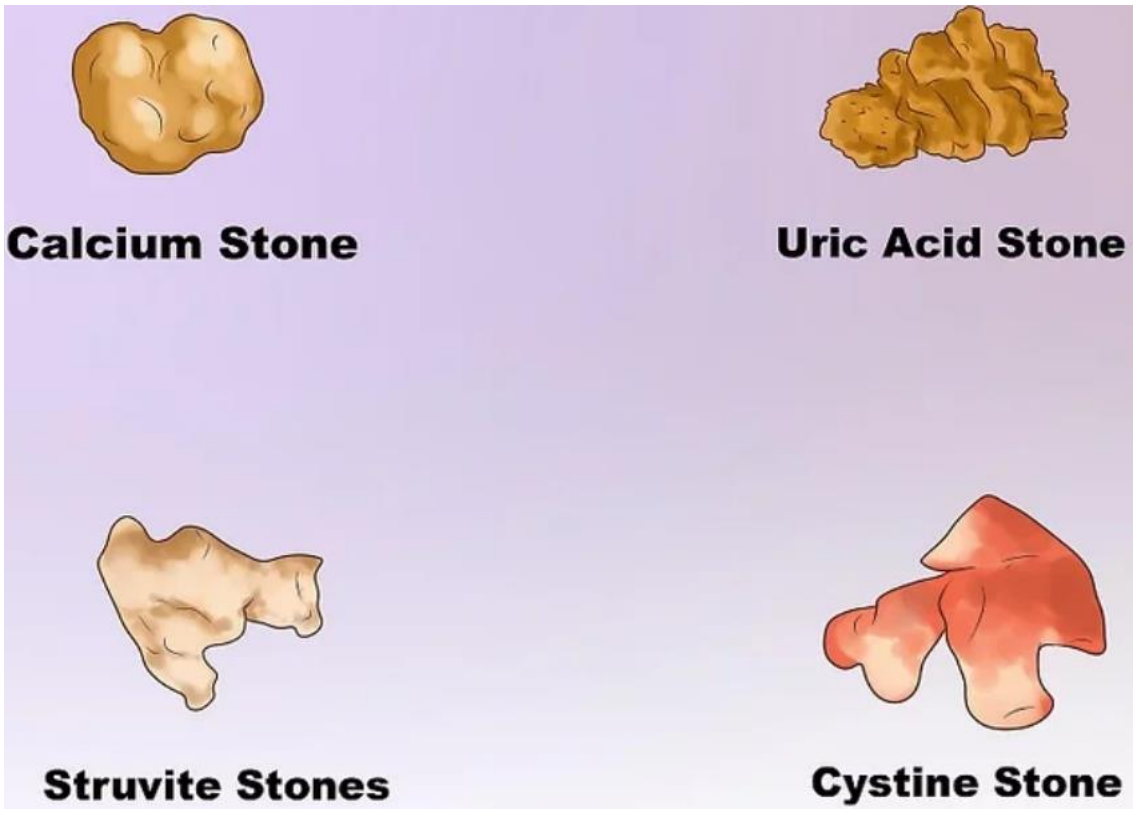

Figure 1.6. Examples of kidney stones.

In the same way, it is possible to classify kidney stones into main types and define origin, incidence and composition (Table 1.2), as shown by Grases *et al.* (2002).

To these data must be added the calculations of rare origin (incidence 1-2%) that can be caused by the accumulation of xanthine, hypoxanthine, cholesterol, fatty acids or 2,8-hydroxyadenine.

Another way of classifying the different types of renal calculi is independently of the chemical composition. The stones can be separated into two large groups: those formed above the kidney wall (especially the papilla), which will be referred to as papillary stones, and the stones that have developed in a kidney cavity, and these will be referred to as cavity stones (Figure 1.7).

Table 1.2. Kidney stones: origin, incidence and composition.

Calcic	**Mixed**	**Uric**	**Infective**	**Cystic**
70 – 80%	5 – 10%	5 – 15%	10 – 15%	1 – 2%
Calcium oxalate (80%)	Calcium oxalate, uric acid and calcium phosphate (30%)	Uric acid, calcium urate	Struvite (phosphate – ammonium – magnesium)	Cystine
Calcium oxalate and calcium phosphate (30%)			Struvite and apatite carbonate or ammonium urate	
Calcium phosphate (10%)			Calcium phosphate	

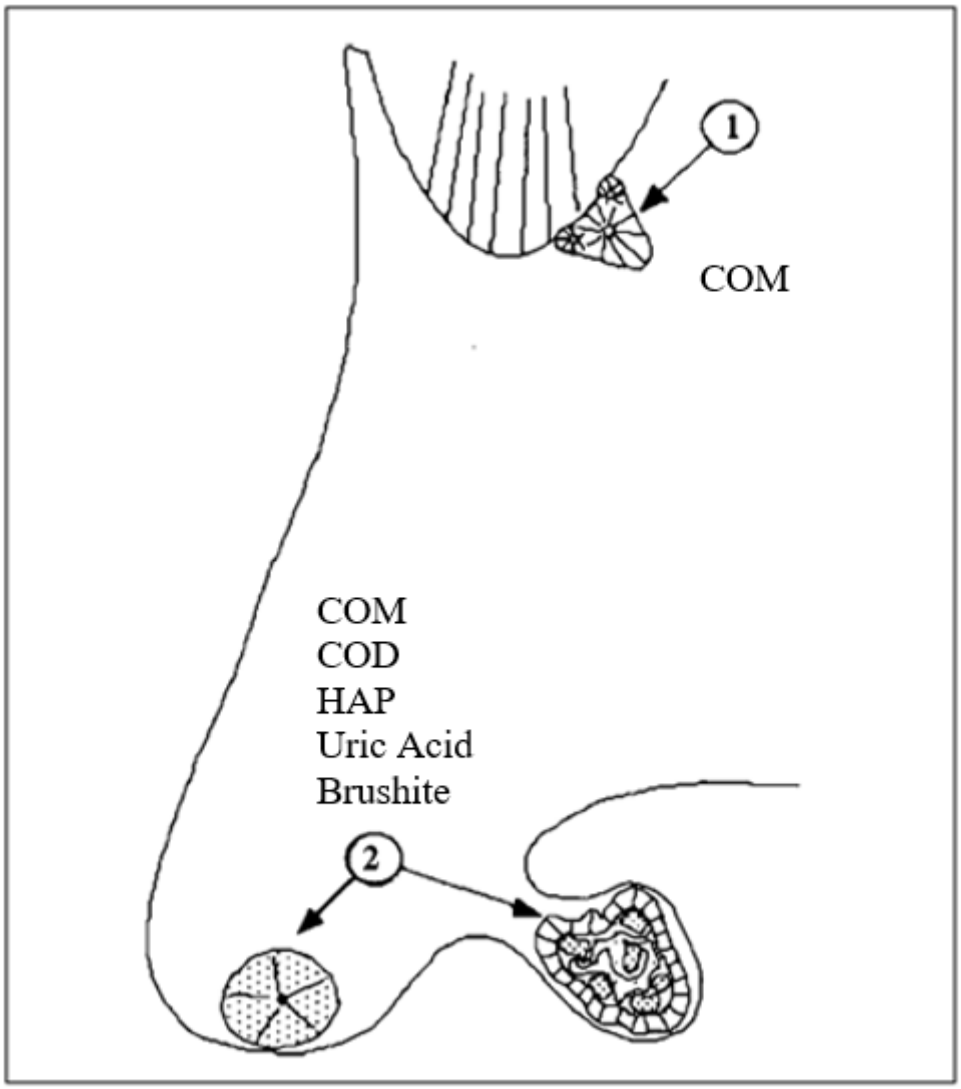

Figure 1.7. Schematic representation of the kidney and position of formation of anchored - papillary - (1) and non-anchored stones - lower calyx or cavity with low urodynamic efficiency - (2).

Every papillary stone clearly shows a union point in the kidney wall, in opposition to what happen with cavity stones. (Grases, 2001).

The place of formation of the stone suggests that a different mechanism of formation takes place: while in the papillary ones it is assumed there is an injury of the uroepithelium of the renal papilla, which allows the crystallization and the deposit of organic substances that form a nest or the heart of what will be the guide for the posterior growth of the calculi, in the cavity ones it is supposed there is a cavity of low urodynamic effectiveness, which translates into a greater residence time of the urine in the kidney, allowing the formation of a nest or the heart that will later grow.

1.6 Physicochemical aspects of urolithiasis

Stones formed in the urinary tract are usually and predominantly crystalline, with the exception of rare matrix stones.

Main process involved in urolithiasis is crystallization, which concerns a transition of phase from liquid to solid. During this change, compounds dissolved in a solvent solidify, arranging themselves according to crystalline structures. From a physical point of view, it is therefore a transformation that implies a decrease in entropy.

1.6.1 Supersaturation

Regardless of where the uro – crystallization takes place or regardless of the chemical nature, the fundamental requirement to drive the reaction is a sufficient free energy, which occurs only when the solution is supersaturated. Furthermore, the energy to be overcome in order to start the crystallization is different than the one needed to sustain this process: in fact, the first is higher than the second.

The term supersaturated refers to a solution in which the concentration of the species that crystallize is higher than its solubility in the solution itself and, in most cases, this is a necessary but not sufficient reason for the formation of stones.

As later explained, the supersaturation can be described in different ways: one of them, is the product between the solubility product (which indicates the maximum soluble concentration of a substance in the considered medium) and the ionic activity of the substance itself, which depends on different factors, like the charge of the ions, the ionic strength of the urine. Also, the temperature of the urine must be taken into account, but it is possible to consider all these factors as constants (Boistelle, 1985).

When the supersaturation is higher than 1, the solution can be considered as supersaturated in relation with the studied substance and, starting from this phase, the substance is capable of crystallize, as shown in Figure 1.8. Notwithstanding, as later shown, the kinetics is strictly connected with the level of saturation (Boistelle, 1985).

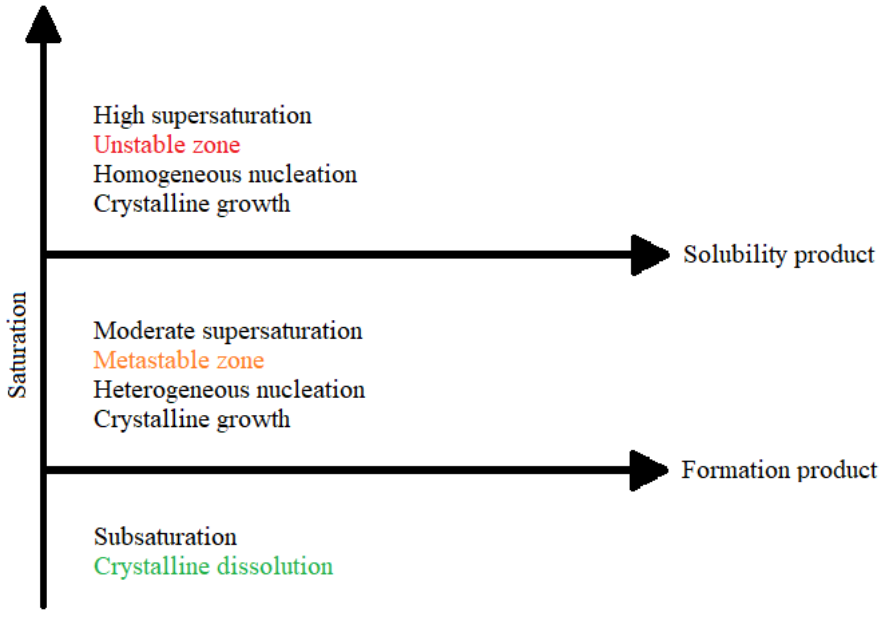

Figure 1.8. Levels of saturation and consequences on crystallization (adapted from Daudon, 2014).

In Figure 1.8, other than the solubility product, also the formation product is considered: it is the lower level of supersaturation that allows the rapid development of crystals, which in this study case correspond to the passage of urine through the nephron. It becomes clear how

can be useful to distinguish the formation product related to the case of the crystallization in the kidney and in the bladder: in the first case, urine remains just for a little time while, in the second case, the urine remains for a little longer period of time (thus, the formation product is smaller).

Supersaturation becomes fundamental: hen it is low, the time required for the formation of a crystalline germ is usually longer than the residence time of the urine in the urinary tract. The higher the level of supersaturation is raised, the more the crystallization kinetics accelerates and the greater the number of crystals formed per unit time. In parallel, the number of molecules necessary for the formation of a crystalline germ decreases (Boistelle, 1985). In other words, the crystals formed in a state of high supersaturation are, on average, more numerous but smaller than those observed in conditions of lower supersaturation (Daudon, 2014).

Between the solubility product and the formation product, the urine is referred to as metastable. It is related to heterogeneous nucleation phenomena, that is, nucleation induced by another previously crystallized species. Instead, it is unfavourable to spontaneous crystal nucleation. This zone corresponds to irregular lithogenic situations that result from multiple supersaturations, such as those observed in calcium or common uric lithiasis, where variations in supersaturation largely depend on environmental factors such as water intake and eating habits.

With saturations higher than the formation product, the urine is considered unstable. The crystallization of the supersaturated species occurs by homogeneous nucleation without the intervention of other factors. Therefore, it is especially in the field of lithiasis associated with genetic diseases (Daudon, 2014).

Finally, condition of sub-saturation is what treatments and therapeutic methods aim to, as it refers to the dissolution of the substances that may form crystals.

Supersaturation needs to be evaluated for each crystallizable species in the urine in an independent way and is always present and usually higher in patients that suffers from the presence of stones (Robertson *et al*., 1968). One reason may be that these patients tend to excrete more amounts of calcium, while another one may be that urinary oxalate can be increased (Marshall *et al*., 1972). Ammonium urate and sodium urate can supersaturate urine (Robertson *et al*., 1972) while, on the other hand, the degree of supersaturation of magnesium ammonium phosphate can happen due to the production of ammonium by bacteria that make the urine alkaline (Robertson *et al*., 1976).

1.6.2 Crystallization

The whole crystallization process is composed of different phases that take place almost subsequentially after the reaching of the condition of supersaturation; they are (in order): crystal nucleation, crystal growth and crystal aggregation. They are shown in Figure 1.9.

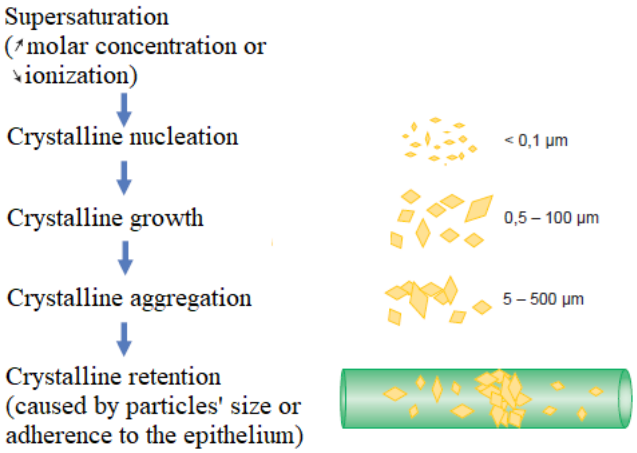

Figure 1.9. Main phases of the lithogenesis (adapted from Daudon, 2014).

The first stage, nucleation, is about the formation of small nuclei of crystal. They are formed of a slight number of atoms that, though, influence only for a small part on the total volume or mass of the crystal.

Primary nucleation, which is defined as the nucleation that happen when there are not other nuclei that form a pre-existing crystal, can be divided in two other subgroups: the homogeneous and heterogeneous nucleation. Homogeneous nucleation occurs in a spontaneous way, when the supersaturation is plentiful, but this almost never happens, as there are always foreign particles or surface imperfections that play a key role in the formation of a crystal. In fact, heterogeneous nucleation occurs at the surfaces of a foreign container or body. In urine, nucleation is basically heterogeneous, if there are no other preformed crystals.

Crystal growth is the step on which is centred this work: it refers to the incorporation of molecules (in this case, ions) from the solution to the crystal lattice and it is the main contributor to the volume or the mass of the crystal. Without this step, stones will not surely form.

Aggregation refers to the fact that crystals bring themselves together and consolidate into a polycrystalline body. Even though this step is what mostly allows the increasing of the average particle volume, as all the stages of crystallization take place almost at the same time, they all influence and cause changes in volumes and numbers of particles (Zauner and Jones, 2000).

All the steps, so the complete process itself, depend for a huge amount on the supersaturation.

1.7 The role of inhibitors and promoters in the formation of urinary stones

Presently, there are three main important mechanisms in the formation of stones in the urinary tract: the first one, as said before, is the supersaturation or, in other words, the relationship between the concentration of the precipitating solute in a solution and the solubility of the forming mineral phase. The other two are the roles of promoters and inhibitors of the crystallization process.

Even though urinary stones are mostly formed by a mixture of different kinds of urinary stones, the main sparingly soluble salt that starts the nucleation in the urinary tract is calcium oxalate; sometimes, it can be calcium phosphate too. Almost daily, the urine is supersaturated with this salt, but not everybody suffers of this mentioned illness.

This is possibly due to high and low molecular weight components (molecules or ions) that can have two specific functions: they can inhibit the formation of nuclei or, if nucleation has already started, they can stop or prevent growth or aggregation or, in other words, an enlargement considerable enough to block the renal collecting tubules. These molecules may also be occluded within the bulk of the calculi and may have the function of supporting intra-renal dissolution or degradation or they may influence the attaching of the calculi to the renal epithelium too. In the shown cases, it is possible to talk about inhibitors.

Among the inhibitors of the crystal's growth, it is possible to include magnesium, citrates, pyrophosphates and zinc, which are small molecules of similar dimension of the ions constituting the crystals.

Furthermore, the inhibitors of the crystal's aggregation, that is the union of single and already formed crystals, are usually bigger and more elongated molecules than the others above – mentioned, as they can lay down on the crystals causing their covering and camouflaging their structure. These substances are usually acid mucopolysaccharides, mucoproteins and RNA – like substances.

The promoters of nucleation of kidney stone are, instead, the main components of the calculi themselves, as they are the substances that tend to precipitate and to form, indeed, crystals, if in condition of excessive concentration: among them, the most important are the oxalate, the ammonium, the calcium and the uric acid (E.M.I., 1988).

Some proteins can be mentioned too, as it was studied that they can bind calcium and induce calcification in vitro under certain conditions (Boyce *et al.*, 1954). Furthermore, proteins are increased in amount and are qualitative different in urine samples from stone – formers than in that from normal people (Boyce *et al.*, 1962).

1.8 An engineering point of view

Human body and its primary physiological functions can be seen as an "industrial palace" or, in better words, as what chemical engineers would see as a chemical plant. (Debschitz et al., 2009). This means that the human body is studied as a complex assemblage of reactors and processing units that exchange mass and energy among themselves and the environment: in order to maintain their functions and to preserve the constancy of internal conditions and environment, physical-chemical transformations are carried out by producing and consuming of energy.

The use of mathematical tools in defining this perspective is not new, but only recently it has been realized the real benefit coming from this point of view, as it can serve as a foundation to analyse, design and control at an "organism level". This kind of approach is an actual way to developing new processes, improving efficiency, understanding, exploring.

In 1983, Grosman and Morari defined the operability as "the ability of a chemical plant to perform satisfactorily under conditions different from the nominal design conditions". This implies that internal and external environments are expected to undergo variations which should not lead to significant deviations. The objectives, in this sense, are:

- Defining steady states for a range of different feeds conditions and plant parameters variations (intended, respectively, as external changes and internal fixed values).
- Fast and regular adaptation and recovery from process disturbance.
- Safe operations, in case of equipment failing.

- Easy start-up and shutdown.

Detection, diagnosis and correction of deviations from the steady state operation of a chemical plant is a critical challenge, because the effects of these variations can be present and lethal even when the plant is normally operating, and this goes for the reaction of human body to illnesses and diseases, too. It is starting to be clear how the analogy between human body and a chemical plant is, actually, strong and effective (Androulakis, 2014).

While diagnosis of a disease may not have been described using terms such as abnormal event and the corresponding treatment may not be considered an event management, the reality is that physicians recognize illness by observing changes, or lack of changes, in vital sign patterns (Buchman, 2010). Still, the problem is that observing the state of a patient means recording an almost infinite number of high-dimensional space attainable from a myriad of initial conditions, that are already past history. Model based approach can be a promising attempt to define and solve this problem.

2. Objectives

In this final master thesis, an investigation on the lithiasis will be developed and a simple kinetic model for the description of the crystallization of kidney stone will be proposed.

Currently, for the diagnosis and the treatment of lithiasis, blood and urinary images and/or analytical examinations are performed. However, the concentrations obtained in the analyses correspond to the time of their extraction and recollection and not of the time of the stone's formation, therefore they may be not of considerable use, especially in the case of idiopathic patients.

Even though the great progress on the investigation of this pathology, the exact sequency of physical-chemical and biologic processes that lead to the formation of urinary calculi is unknown. The stone is the only permanent testimony of the lithiasis and of all the events that lead to its genesis and formation are impressed in its own structure.

Because of this reason, in this work it is proposed the design of a new method of characterization of the calculus. More precisely, in order to analyse the renal calculi that have been extracted by chirurgic operations, the Scanning Electron Microscopy with Energy Dispersive X-Ray (SEM-EDX technique) has been used. A morpho-constitutional analysis has been performed by following a radial trajectory (from the periphery to the nucleus) in order to determine the different layers that form the stone and establish a scheme of events related both to the growth of the stone and to the urinary biochemical cycle.

Final objective of this work is establishing a time scale of the growth lithic processes, in order to be able to study the chronology of the different chemical and clinical events that caused the pathology.

The electrochemical microenvironment effect on the solutes distribution will be studied, as it may notably alter ions concentration. More precisely, the proposed flux model will be depending on the effect of supersaturation and on the mass transfer coefficient, considered as the most fundamental factors.

The supersaturation will be described taking into account the influence of several important factors, which are the ionic concentration and the electrochemical potential. Instead, the mass transfer coefficient will be dependent on the Reynolds number, which means that the flux in the kidney will be considered.

Furthermore, a urinary cavity calculus will be analysed in order to study the concentration variations of the most important compounds.

A circadian biochemistry will be proposed, by previously mathematically identifying the cycle time and the maximum concentration.

The predictions will be adjusted on the SEM-EDX results, by differentiating the case of the cavity stone and the papillary stone.

This work has been in collaboration with the Sanitary Investigation Institute of Biocruces (Bizkaya, Basque Country) and the Hospitals of Cruces (Bizkaya, Basque Country) and Basurtu (Bizkaya, Basque Country) through the "ALIRE" project.

3. Theoretical kinetics background to build up the mathematical model

Apart from sporadic matrix stones, the majority of stones in the urinary tract are primarily crystalline. Crystallization is an extensively studied physicochemical process that involves a change of phase and different steps.

First of all, in order to take place, regardless of the chemical nature and of the environment, an energy barrier needs to be overcome and this means that it is essential the presence of a sufficient free energy to drive the reaction. This happens when the concentration of the species that is going through crystallization in the solution is greater than its solubility value in the mentioned solution. In other words, this happens when the system is supersaturated.

The most important stages of the crystallization process are nucleation, crystal growth and crystal aggregation. Nucleation is the initial event: during this step, small crystal nuclei are formed. Instead, during crystal growth, molecules or ions from the solution are incorporated in the crystal lattice: this is the most relevant contribution to the final mass and volume of the complete stone. Finally, aggregation is the union and the consolidation of single separated crystals into a one polycrystalline body.

This work focuses its attention on the crystal growth step and on the modelling of a plausible kinetic equation that may describe this stage. In order to do as pointed out, the theoretical background will be explained.

3.1 Enthalpy in chemical reactions

Thanks to chemical thermodynamics, it is possible to study the thermal effects of chemical reactions: these are the heats of reactions. Thus, this branch of thermodynamics allows to quantify and calculate the absorbed or released during a chemical reaction and it concerns the conversion of chemical energy in thermal energy and vice versa by studying the variables connected to them (like standard formation enthalpy and binding energy).

The entire subject is ruled by two important laws:

- Lavoisier and Laplace Law (1780), which states that the transfer of heat during a certain chemical reaction is equal and opposite to the transfer of heat in the contrary direction;
- Hess Law (1840), which affirms that the variation of the enthalpy of reaction is the same, regardless of the number of the consecutive independent stages (even purely hypothetical).

It is possible to deduce empirically these laws from the first principle of thermodynamics and are direct consequences of itself (Atkins P.W., 1999).

More precisely, as shown in Equation (3.1), keeping into account the stoichiometry of the reaction, the variation of enthalpy can be defined as the difference between the enthalpies of the products and of the reagents.

$$\Delta H = H_{products} - H_{reagents} \tag{3.1}$$

The shown variation of enthalpy can be positive or negative, depending on the reaction itself and on the energy contained in the products: if during the reaction the heat is absorbed

and the products contain more energy than the reagents, then the reaction is endothermic and the enthalpy H increases with the evolving of the reaction, which means that the variation is positive. When heat is released during the reaction, it is possible to observe an opposite situation, and the reaction is defined as exothermic. It is possible to see the difference in Figure 3.1.

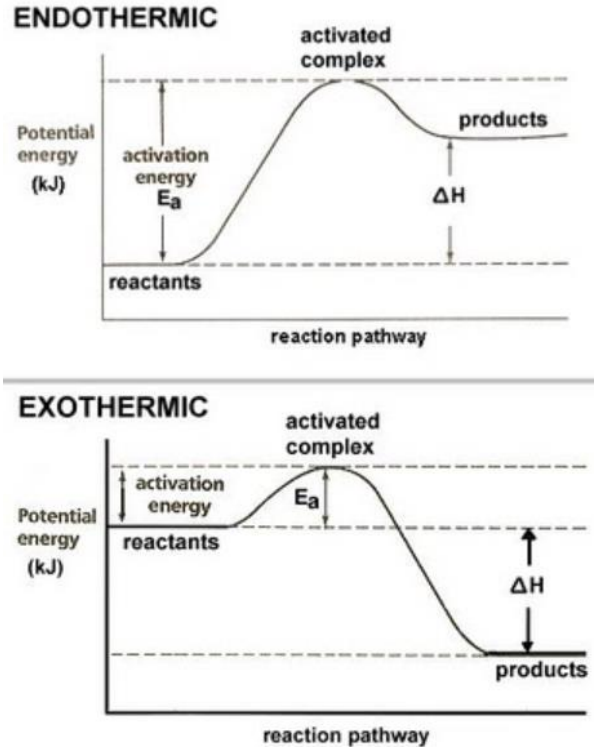

Figure 3.1. Variation of enthalpy for an endothermic and an exothermic reaction (adapted from Klein, 2018).

For an exothermic reaction, the formation of products is promoted by reducing the temperature, while for an endothermic reaction, the formation of products is supported by increasing the temperature.

This is important as all physicochemical environment factors affecting crystallization combine properly in the urinary system, making crystal growth a favourable process.

From the tabulated values of the enthalpies of formation of the compounds implied in the evolution of kidney stones, it is possible to evaluate the heat of the reactions whose reagents are the mentioned compounds. These values are at standard conditions, which means a temperature of 25 °C and a pressure of 1 atm, but these are not the conditions in the growth environment of kidney stones; a modification is needed, in order to evaluate a solubility constant at the real conditions of the urine. Said constant will be useful in the evaluation of supersaturation.

3.2 Solubility constant and Van't Hoff Equation

The solubility constant (or solubility product), indicated with K_{sp}, is a measure of the solubility of a compound and it is generally expressed with molar concentrations. It corresponds

to the equilibrium constant of the hydrolysis reaction of the compound, being the concentration of the solid material a constant, thus included in the equilibrium constant K_c.

As a result, this constant is often represented with the product of the concentration of the ions that the compound forms during dissociation: each concentration is raised to a power equal to the coefficient with whom the ion appears in the reaction.

For example, given the following reaction in the Equation (3.2):

$$A + bB \leftrightarrow cC + dD \tag{3.2}$$

The solubility constant would be as shown in Equation (3.3):

$$K_{sp} = \frac{[C]^c[D]^d}{[A]^a[B]^b} \tag{3.3}$$

As an equilibrium constant, the solubility product depends on temperature. It is evaluated at constant pressure (1 atm) and temperature (25 °C).

As previously mentioned, the condition of temperature in the urine is quite different than the standard conditions at which the solubility constant is calculated, thus it is possible to obtain the real value of the solubility constant, which means at different conditions from the standard ones, by using the Van't Hoff equation.

Van't Hoff equation is a mathematical relation that expresses linearly the variation of the equilibrium constant of a chemical reaction as a function of the changes of temperature. This can be applied when the pressure is constant and if the variation of the enthalpy of reaction can be considered independent from the temperature itself.

By considering constant the variation of the entropy of reaction and the variation of the free energy of reaction in the studied temperature range (25 °C – 37 °C), it is possible to finally obtain the equation shown in (3.4):

$$\ln\frac{K_2}{K_1} = \frac{\Delta H_r^\circ}{R}\left(\frac{1}{T_1} - \frac{1}{T_2}\right) \tag{3.4}$$

Where:

- K_2, K_1: value of the equilibrium constant for temperatures T_1 and T_2;
- T_1: reference temperature (298.15 K, which means 25 °C);
- T_2: process temperature (310,15 K, which means 37 °C);
- R: ideal gas constant (8.314 J/molK);
- ΔH_r°: enthalpy of reaction when both reactants and products are in their standard state and at 25 °C (298.15 K).

The expression 3.4 can only be applied if the pressure is constant and the enthalpy of reaction is independent from the temperature.

It can be useful to express the solubility constant with activities, in order to better point out the effective compounds taking part in the reactions. In terms of activities, for every kind of reaction, the solubility constant will be expressed as in Equation (3.5):

$$K_{sp} = \left(\frac{activities\ of\ the\ products}{activities\ of\ the\ reagents}\right) \tag{3.5}$$

Thus, for the generic reaction shown in Equation (3.2), the solubility constant can be written as shown in Equation (3.6).

$$K_{sp} = \frac{a_C^c a_D^d}{a_A^a a_B^b} \tag{3.6}$$

The same previous expression is valid for heterogeneous equilibrium, like kidney stones in urine.

3.3 Expression of coefficients of activities: limiting law of Debye - Hückel and Davis equation

Due to the forces of attractions, the ions in a solution do not behave in an ideal way, as these forces impede a number sufficiently elevated to be independent from one another. Hence, not every ion derived from the dissociation of the solute can participate a given phenomenon as an equilibrium or a kinetic process, so the active mass of the solute (indeed, the activity) is lesser than the initial analytic concentration.

Between the molar concentration of a solute and its activity, there is the relation shown in Equation (3.7):

$$a = \gamma C \tag{3.7}$$

Where γ is the coefficient of activity of the solute. The activity is a pure number; therefore, the coefficient of activity has the inverse of concentration as a unit of measurement.

In order to evaluate the coefficient of activity of a given solute, the limiting law of Debye - Hückel in its extended form can be used (Equation 3.8):

$$-\log\gamma_i = \frac{z_i^2 q^3 N_A^{1/2}}{4\pi(\varepsilon_r\varepsilon_0 k_b T)^{3/2}}\sqrt{I\frac{10^3}{2}} \rightarrow -\log\gamma_i = Az_i^2\sqrt{I} \tag{3.8}$$

A is a constant that gathers all the other constants present in the Equation (3.8) and has the following form (Equation 3.9):

$$A = \frac{q^3 N_A^{1/2}}{4\pi(\varepsilon_r\varepsilon_0 k_b T)^{3/2}}\sqrt{\frac{10^3}{2}} \tag{3.9}$$

The ionic force is expressed as I, and it is the summation of the concentrations of the solutes multiplied for the square power of the charge of their ions (Equation 3.10):

$$I = 0.5\sum_i z_i^2 C_i \tag{3.10}$$

Generally, the equation of Debye - Hückel does not fit much when the molarity is greater than 0.1 for an electrolyte 1:1 (as the difference between the calculated value and the measured one is around 2%).

This means that the calculations become less precise for electrolytes that dissociate into ions with higher charges. In this case, the Davis modification of the Debye - Hückel equation can be used; for individual ions, this is as shown in Equation (3.11):

$$\log\gamma_i = -0.523 z_i^2\left[\left(\frac{I^{1/2}}{1+I^{1/2}}\right) - 0.3I\right] \tag{3.11}$$

The factor 0.523 is a temperature dependent constant (for 37 °C) and 0.3 is the usual empirical constant. The equation in (3.11) is approximately valid for I up to about 0.2 mol/L.

Addition of electrolytes can change the solubility: if it increases, it is referred as "salting in", while if it decreases, it is referred as "salting out". For calcium salts in urine, the effects of ionic strength and complex formation will generally lead to salting in (Grover et al., 2003).

3.4 Supersaturation equations: the real driving force of crystallization

Physicochemical aspects and features of urolithiasis (that are nucleation, growth and aggregation) are interrelated subjects depending on one main factor defined as the chemical driving force of the phenomenon of stones formation, which is urinary supersaturation of salts or solutes promoting the formation of crystals (Finlayson B., 1978; María *et al*., 2019).

The most important factors that determine the supersaturation level are (Gómez Ayala, 2015):

- Urinary pH;
- Ionic strength;
- Solute concentration;
- Degree of composition or formation of complexes with other ions.

Taking into account that the higher the concentration of two ions, the greater the probability that they will precipitate. Thus, if the solubility product (K_{sp}) is exceeded, the process of crystallization and heterogeneous nucleation can start.

There are several ways to express supersaturation and all of them entail the concentration of the crystallizing species in the solution and the solubility of the species (such as the concentration in the solution, which is in equilibrium with crystals).

In fact, the first way to express supersaturation Γ is as the ratio between the concentration of the compound in the solution and the concentration of said compound at equilibrium (Equation 3.12):

$$\Gamma = \frac{C_s}{C_{eq}} \tag{3.12}$$

It is possible to define the relative supersaturation σ (Equation 3.13):

$$\sigma = \frac{C_s - C_{eq}}{C_{eq}} = \frac{\Delta C}{C_{eq}} \tag{3.13}$$

When the crystallizing species is a salt (i.e. calcium oxalate), the concentration in Equation (3.13) are replaced with the product of them. These concentrations are just like the effective ones of the relevant species that are the decisive factors in crystallization.

This implies that they are coincident with the activities and this distinction is even more useful when other salts are present, like in the case of urine, since the solubilities can considerably vary.

Hence, in terms of activities, it is possible to obtain the following equations (from 3.14 to 3.18).

$$\Delta a = a_s - a_{eq} \tag{3.14}$$

$$\Gamma = \frac{a_s}{a_{eq}} \tag{3.15}$$

$$\sigma = \frac{a_s - a_{eq}}{a_{eq}} = \frac{\Delta a}{a_{eq}} \rightarrow \sigma = \Gamma - 1 \tag{3.16}$$

$$\Gamma = \frac{K_{sp,sol}}{K_{sp,eq}} \tag{3.17}$$

$$\Gamma = \left(\frac{\prod_i a_i^{m_i}}{K_{sp}}\right)^{1/n} \tag{3.18}$$

The definition of supersaturation in terms of activities derives from physicochemical considerations of chemical potential of the considered substance, both in solid (crystal) form and in solution state.

Mijangos *at al*. (2020), like Kavanaugh (2006) before, cleared how the first stone, in order to form and not dissolve or be removed by the urinary system, needed to overcome a force that inhibits aggregations: this is a repulsive electrostatic surface charge, known as zero potential. A consequence of this discussion may be that the prime crystallization driving force is the difference of chemical potential in the liquid supersaturated state and solid state.

In equilibrium conditions, chemical potentials in liquid state and solid state have the same value; in the case of urine, these are different and the chemical potential of the solute in the crystal is considered as the chemical potential of the solute in the solution at equilibrium.

It is possible to express the pointed-out difference as in Equation (3.19):

$$\Delta\mu = \mu_s - \mu_{eq} \tag{3.19}$$

Crystallization occurs when $\Delta\mu < 0$.

Since constant pressure and temperature are assumed during the time of the taking place of the reactions, it is possible to relate what said so far with Gibbs free energy (ΔG): crystallization takes place only when Δμ (then ΔG) are negative.

Chemical potential in a mixture has the expression shown in Equation (3.20):

$$\mu_s = \mu^0 + RT\ln(a_s) \tag{3.20}$$

Combining (3.19) and (3.20), it is possible to obtain the "real" driving force of the process (Equation 2.21):

$$-\Delta\mu = RT\ln\left(\frac{a_s}{a_{eq}}\right) \rightarrow -\Delta\mu = RT\ln\Gamma \tag{3.21}$$

Supersaturation can also be related to the superficial tension of the stone by the Gibbs – Thomson equation that links crystal size with the equilibrium solubility. For an equilibrium between crystal and the solution in which it is present, the concentration corresponding to a specific radius of a spherical crystal is related to the solubility of spherical crystal of infinite size, according to Equation (3.22):

$$\ln\left(\frac{C_{eq}(r)}{C_{eq}(\infty)}\right) = \frac{2\sigma V_m}{RTr} \tag{3.22}$$

Where:

- $Ceq\ (r)$: solubility of spherical crystals of radius r
- $Ceq\ (\infty)$: solubility of spherical crystals of considerably large size
- σ: surface energy of the solid phase
- Vm: molar volume
- R: ideal gas constant
- T: absolute temperature
- r: crystal radius

In this case, regarding the surface energy of the solid phase, it is considered an equilibrium solubility function for a great variety of solid substances, while 2 is a form factor. The equation (3.22) implies that the solubility increases with decreasing crystal size, as the surface tension forces between the crystal and the solution cause a larger solubility of small crystals.

3.5 Crystal growth: Nernst-Planck equation and its solution

The terms "crystal growth" mean the incorporation of substances (such as, for example, ions) and do not necessarily imply growth in terms of size, which can also occur at a later stage, such as aggregation (Rao N.P. *et al.*, 2011).

Furthermore, in order to achieve crystal growth, the main two factors that must be taken into account are the transport of ions or crystallizing component to the surface of the crystal from the solution and their incorporation in the growing structure.

If the rates of these two processes are similar, they both must be taken into account while studying and evaluating the kinetics. If the rates of the two processes are dissimilar, then only the slower one will be the controlling one.

The morphology of the stone shows how growth bands are present, and their width corresponds to precipitation waves and urinary concentration peaks. Thus, the width is independent of radial position, layer and element analysed (Mijangos *et al.*, 2020).

As a consequence, it is possible to conclude that the stone growth is a kinetically controlled phenomenon. In this work, a model to describe crystal growth is proposed and it aims to show the dependence of crystal growth rate on supersaturation and on the principal driving force of the formation of kidney stone, which is chemical potential.

The kinetic growth can be described by taking into account supersaturation, considering as shown in the following equation (3.23):

$$g = k\sigma^n \rightarrow g = k(\Gamma - 1)^n \tag{3.23}$$

Where:

- g: growth rate;
- k: constant;
- n: stoichiometric coefficient that depends on the considered substance (for example, for calcium oxalate CaOx is 2).

Another way to consider the crystal growth, relating it to chemical potential, is moving the discussion at a ions level, in order to model the dynamics of the system by considering it as a multicomponent ion exchange.

To do as mentioned, the Nernst – Planck equation will be used and only the electrostatic migration term will be considered, as it is the limiting step (Equation 3.24):

$$J_i = -D_i \frac{z_i F C_i}{RT} \nabla \varphi_i \tag{3.24}$$

It is possible to relate the flux to the chemical potential by knowing that this depends on the electrostatic potential, based on the relation in the Equation (3.25), and the flux will have the expression in Equation (3.26):

$$z_i F \nabla \varphi = \nabla \mu_i \tag{3.25}$$

$$J_i = -D_i \frac{C_i}{RT} \nabla \mu_i \tag{3.26}$$

Boundary conditions will be as following (Equations 3.27):

$$\mu(r) = \begin{cases} \mu_{i,sol}, & r \to \infty \\ \mu_{i,eq}, & r = R \end{cases} \tag{3.27}$$

Where $\mu_{i,eq}$ is the chemical potential at equilibrium, as in the solid phase.

In order to obtain a flowrate, the specific area will be multiplied both sides and the solution of the equation will be as shown in (3.28):

$$J_i a = -D_i a \frac{C_i}{RT} \Delta \mu_i \tag{3.28}$$

4. Materials and methods

4.1 Analytical techniques for the morpho-compositional study of renal calculi

Since the origin and the whole history of kidney stones are imprinted in their own structure, finding a proper way to study its constitution becomes central in understanding the processes involved in its growth.

Usually, both chemical and physical methods are used to analyse the stone but, unfortunately, chemical techniques are not always accurate enough to allow the detection of some particular elements in the stone and the quantification of them in mixed stones. Furthermore, chemical instruments are not often able to specify and differentiate crystalline phases of calcium oxalate or calcium phosphate. This may be important, because depending on the compounds that actually constitute the stone, it is possible to investigate and recognize the biochemical and pathophysiological condition (Cloutier *et al*., 2015).

Among physical methods, X-ray diffraction (XRD) and Fourier transform infrared spectroscopy (FTIR) are currently used for stone analysis, as they are capable of identifying each of the constituting compound of the stone and can give a semi-quantitative evaluation of their proportion within the stone. Physical methods manage also to grant information on the crystalline phases of the same chemical species, and this imply different lithogenic conditions and processes, such as diet imbalance and genetic or acquired diseases (Daudon *et al*., 2012).

In view of this, only physical methods can identify such diversity of components and achieve such results and goals. Several techniques were explored for this aim, like Raman Spectroscopy (RMN), Infrared Spectroscopy (IR), thermal analysis and even stereomicroscopy for stone morphology. Limitations may be due to costs and the choice of the method can depend on precision and accuracy of the equipments.

4.1.1 Conventional study of a urinary stone

A conventional study for the analysis of a urinary stone involves the use of the following techniques: optical microscopy and infrared spectroscopy (IR). While, in research, the following techniques are also used: X-ray Diffraction (XRD) and/or scanning electron microscopy (SEM) with EDX analysis.

First, with optical microscopy, the external appearance of the stone is observed and, after sectioning it, its internal structure is visualized in order to differentiate, among others, the nucleus and the layers that surround it (Garcia Garcia *et al*., 2011; Ramis *et al*., 2002).

After visualization by optical microscopy, an analysis by Infrared Spectroscopy (IR) is carried out to know the relative composition of each of the components present. X-ray Diffraction techniques (XRD) and Scanning Electron Microscopy (SEM-BSE and SEM-EDX) are used for the detection and identification of substances found in smaller quantities (micro-components) in the stone. Therefore, it is considered that the use of techniques such as scanning electron microscopy, despite its high cost, is decisive to establish the etiology of stone formation (Garcia-Garcia *et al*., 2011; Ramis *et al*., 2002).

4.1.2 Electron microscopy with energy-dispersive X-ray spectroscopy (SEM-EDX)

Indeed, among the majority of exploited techniques, Mijangos *et al.* (2020) used the electron microscopy with energy-dispersive X-ray spectroscopy (SEM-EDX) to obtain a description of the main morpho-compositional aspects of a single bladder stone. This allowed to consider both qualitative and quantitative aspects of the stone structure (including minor components) and to know the distribution of these elements within the stone (and the corresponding morphology), revealing this kind of approach useful to the purpose and adequately complete.

The sample studied was supplied by Cruces University Hospital (Barakaldo, Spain) and it was a bladder calculus from a 74-year-old male stone former, who suffered recurrent urinary infection due to *Staphylococcus aureus*.

For what concerns the microanalysis of the stones, the sample of urinary stone has been put into an epoxy resin block (in order to avoid breaking) and divided into two halves, with the goal to obtain a flat surface. While one half was destined to a chemical analysis with the Raman and Infrared Spectroscopy (IR), the other half was destined to a SEM-EDX linear scanning.

This second open cross-section was sanded with 20 μm diamond plates, smoothed with 3 μm diamond suspension cloths and finally with colloidal alumina (Al_2O_3). In order to obtain microphotographs of the stone that would show and highlight diverse composition areas, backscattered electrons (SEM-BSE) were used.

The scanning is referred to as “linear”, since the trajectory was radial, from the external margin to the nucleus of the stone. The beam surface intensity was between 5 – 10 nA and the longitude of the trajectory was of 2.14 mm.

With this specific kind of linear scanning, it was possible to obtain all the data regarding the elements that constitute the stone in the studied trajectory and adequate information on the composition of the stone itself. In other words, by knowing what is present in the stone, it is possible to understand the chemical environment in which it has grown and the events that gradually led to its expulsion.

In pursuance of the appropriate treatment of the data at the beginning and of the achievement of a suitable kinetic model in this work, many mathematical tools and filters were used. First of all, the EDX quantitative analysis requires a previous calibration with standardized samples but since this could not be obtained due to the absence of those, the data can be read as the relative concentrations of the elements in the stone as a function of the radial position (which is the trajectory of the scanning). This can be realized by considering that the intensity of an X-ray line is approximately proportional to the mass concentration of the element concerned.

The obtained relative concentrations were used in order to evaluate the final kinetic growth model of the stone and the value of the mass transport coefficient.

4.2. Calculations of the deposited mass

As previously mentioned, the morpho-constitutional analysis of urinary stones showed the presence of growth bands and a multi-layered structure. These layers are Liesegang ring-like structures, of which it is possible to reveal the main components as a function of space. Furthermore, each growth band correspond to a urinary concentration peak and a precipitation wave.

In Figure 4.1, the microphotographs of the stone cross-section are shown. It is worth noting that in the right figure the trajectory followed by the linear scan can be recognized, while in the left image all the different layers can be identified: each one of them correspond to the predominant presence of a different element, salt or compound.

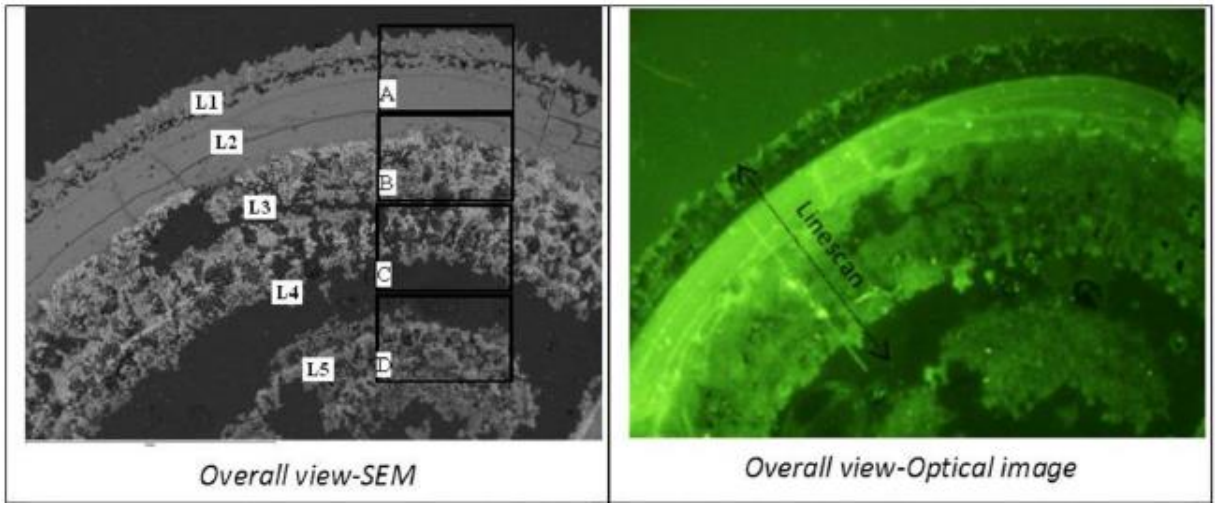

Figure 4.1. Microphotographs of the stone cross-section: on the left, the overall view; on the right, the optical image. Figure from Mijangos *at al*., 2020, "SEM-EDX linear scanning: a new tool for morpho-constitutional analysis of growth bands in urinary stones", *J Biol Inorg Chem*, June 2020.

Based on the methodology of the processing of the samples and their analysis, it has been decided to realize different parallel scans during the SEM-EDX analysis, with the purpose of corroborating the information obtained on the first ones. This decision is due to a variable morphology of the complete surface of the stones. Only the most relevant scans have been taken into account for the analysis.

The first evaluation step is calculating the deposited mass in each layer, considering position and thickness of each layer (which is the width of the growth band).

To do as explained, the geometry of the urinary stone is considered and, more precisely, the particle is considered as spherical.

Also, the longitude of the linear trajectory of the SEM-EDX scanning of 2.14 mm is considered as a complete radial trajectory. This means that the radius of the spherical particle is, actually, equal to 2.14 mm.

Being x_j the mg of the element j on a volume basis (mm^3), it is possible to evaluate it as in Equation 4.1 (knowing that Ct_j is the counts of the considered element j:

$$x_j(r) = k_j Ct_j \tag{4.1}$$

Where:

- $x_j(r)$: mg/mm^3 of each element
- k_j: conversion factor (counts → mass) of each element
- $Ct_j(r)$: counts of each element

Integrating it all over the particle, it is possible to obtain the total mass of the element j (Equation 4.2):

$$m_j = 4\pi k_j \sum_i Ct_i \, r_i^2 \Delta r_i \tag{4.2}$$

By considering the average density of the particle as the weighted average of the components present in it and taking into account the porosity of the stone, it is possible to evaluate the ration between the mass of the component j in the stone and the total mass of the particle as following (Equation 4.3):

$$X_j = \frac{m_j}{m_T} = \frac{4\pi k_j \sum_i Ct_i \, r_i^2 \Delta r_i}{{}^4/_3 \, R_p^3 \rho_p} \tag{4.3}$$

Finally, since the conversion factor does not change with the local density of the crystallized phase but, instead, it remains constant, it is possible to evaluate it for each element as shown in Equation 4.4:

$$k_j = \frac{R_p^3 \rho_p X_j}{3 \sum_i Ct_i \, r_i^2 \Delta r_i} \tag{4.4}$$

To sum up everything that has been stated so far, with this study, it has been possible to evaluate the conversion factor k_j for each element, that allows to convert the counts into mass.

For the exact purpose of realizing the study, the main characteristics of the sample are taken into account and shown in Table 4.1.

Table 4.1. Data of the chosen stone's patient and of the stone itself.

Radius (mm)	Volume (mm^3)	Weight of the stone (gr)	Porosity
2.14	41.05	84.01	5

By using the Table 4.2. (from Mijangos *et al.*, 2020), where the percentage of each crystalline species is shown, it is possible to evaluate de elemental composition of the renal stone for the majority of the elements (like carbon, calcium, potassium and so on).

Table 4.2. Percentages of crystalline species in the urinary stone

Compound name	Abbreviation	Chemical formula	Semi-quantitative percentage [%]	Molecular weight (g/mol)	Density (kg/m^3)
Weddellite	COD	$CaC_2O_4 \cdot 2H_2O$	17	164,13	1,94
Whewellite	COM	$CaC_2O_4 \cdot H_2O$	50	146,11	1,94
Struvite	ST	$Mg(NH_4)PO_4 \cdot 6H_2O$	13	245,11	1,71
Hydroxyapatite	HAP	$Ca_5(PO_4)_3OH$	20	502,31	3,16

By knowing the percentages of every species in the stone and by using the density of every crystalline compound, it is possible to calculate the density of the stone, also considering a mineral intrusion of the 5%. Finally, it is possible to obtain the results shown in Table 4.3.

Table 4.3. Densities of the porous and solid stone.

	Density (kg/m3)
Pure and solid stone	2,15
Real porous stone	2,05

To the extent of knowing the proportion of each element in the solid and porous stone, in the first step it is required to evaluate the elemental percentages. As an example, the calculation of the elemental percentage for the COM is detailed below.

- Calcium

In 1 mole of COM, 1 mole of Ca is available, so that the mass of Ca is obtained (Equation 4.5):

$$moles = \frac{mass}{molecular\ weight} \rightarrow 1mol\ Ca = \frac{mass\ of\ Ca}{40{,}01} \rightarrow mass\ of\ Ca = 40{,}01\ gr \quad (4.5)$$

Knowing the molecular weight of COM, the mass of COM is obtained (Equation 4.6):

$$mass\ of\ COM = 1\ mol\ x\ 146{,}11\ \frac{gr}{mol} = 146{,}11\ gr \quad (4.6)$$

Which means being able to evaluate the percentage of Ca (Equation 4.7):

$$\%\ Ca = \frac{mass\ of\ Ca}{mass\ of\ COM} x\ 100\% = 27{,}43\ \% \quad (4.7)$$

- Oxygen

In 1 mole of COM, 5 moles of O are available, so that the mass of O is obtained (Equation 4.8):

$$moles = \frac{mass}{molecular\ weight} \rightarrow 5mol\ O = \frac{mass\ of\ O}{16} \rightarrow mass\ of\ O = 80\ gr \quad (4.8)$$

Which means being able to evaluate the percentage of O (Equation 4.9):

$$\%\ O = \frac{mass\ of\ O}{mass\ of\ COM} x\ 100\% = 54{,}75\ \% \quad (4.9)$$

- Hydrogen

In 1 mole of COM, 2 moles of H are available, so that the mass of H is obtained (Equation 4.10):

$$moles = \frac{mass}{molecular\ weight} \rightarrow 2mol\ H = \frac{mass\ of\ H}{1} \rightarrow mass\ of\ H = 2\ gr \quad (4.10)$$

Which means being able to evaluate the percentage of H (Equation 4.11):

$$\%\ H = \frac{mass\ of\ H}{mass\ of\ COM} x\ 100\% = 1{,}38\ \% \quad (4.11)$$

Once the calculation methodology is known, the elemental percentage is calculated in each of the compounds and, in turn, in the solid and porous stone. Table 4.4 summarizes the results obtained.

Table 4.4. Elemental percentage in each crystalline species and real elemental percentage in the kidney stone studied.

	Elemental %						
Compound	**Calcium**	**Hydrogen**	**Carbon**	**Oxygen**	**Magnesium**	**Phosphorus**	**Nitrogen**
COM	27,43	1,38	16,44	54,75			
COD	24,42	2,46	14,64	58,49			
ST		6,57		65,2	9,9	12,62	5,71
HAP	39,89	0,2		41,41		18,5	
Pure solid stone	25,84	2,00	10,71	54,08	1,29	5,34	0,74
Porous real stone	24,55	1,9	10,17	51,37	1,22	5,07	0,71

Subsequently, the results of the k_j for the main components of the stone are shown in table 4.5.

Table 4.5. Estimation of k_j coefficients to convert counts/seg to mg/cm^3

Element	**Chemical formula**	**% estimated in the pure stone**	**% expected in the real stone**	**Sum counts/s**	**k_j**
Carbon	C	10.71	10.17	8.60E+04	8.32E-06
Calcium	Ca	25.84	24.55	1.45E+05	1.19E-05
Phosphorus	P	5.34	5.07	8.46E+04	4.22E-06
Chlorine	Cl	3.05	2.90	2.60E+04	7.86E-06
Oxygen	O	54.08	51.37	3.16E+04	1.14E-04
Sodium	Na	1.66	1.57	9.15E+03	1.21E-05
Magnesium	Mg	1.29	1.22	8.75E+03	9.84E-06
Potassium	K	0.55	0.52	9.32E+03	3.96E-06
TOTAL		102.52	97.39		

Ultimately, the estimated values of concentration in mg/cm^3 of the main components are shown in table 4.6.

Table 4.6. Estimated concentrations (mg/ cm^3).

Element	Chemical formula	Maximum value	Minimum value	Average value
Carbon	C	241	1	49
Calcium	Ca	500	5	264
Phosphorus	P	133	0	35
Chlorine	Cl	32	2	13
Oxygen	O	2497	8	493
Sodium	Na	37	0	11
Magnesium	Mg	23	0	9
Potassium	K	8	1	4

Analyzing the results cited in Table 4.6, it can be seen that the amount of carbon, calcium and oxygen is considerably higher than that obtained in the rest of the elements detected. This agrees with the estimated proportion in Table 4.2, where 50% of COM was expected.

Furthermore, it is possible to evaluate the concentrations of oxygen, hydrogen, nitrogen and magnesium in the external layer.

For the oxygen, its concentration has been evaluated by keeping into account that they are present in the form of oxides (in this case, the calculations were determined by considering the atomic balances).

Additionally, also the concentration of nitrogen in the form of struvite in the external layer was calculated; it has been proved that its concentration is equal to the one of the magnesium, because of the stoichiometry of the chemical formula of the struvite itself.

Lastly, the concentration of hydrogen has been calculated too and it has been highlighted that its total concentration is the 2% of the total sum of concentrations present in the stone.

The above is summarized in table 4.7.

Table 4.7. Continuation of the estimated concentrations (mg/cm^3).

Element	Chemical formula	Maximum value	Minimum value	Average value
External Oxygen	O	888	53	435
External Nitrogen	N	14	0	5
External Magnesium	Mg	14	0	5

External Hydrogen	H	60	2	18
TOTAL SUM		3057	81	903

4.3. Circadian cycle-based time trend

In figure 4.2., it is possible to observe the trend of the concentration of calcium (blue line) and the trend of the concentration of sodium (orange line) as a function of the radial position. The choice of representing the trends of these two components is not random or accidental: in this way, it is actually possible to clearly visualize the difference between the concentration of a majority and minority components and also to understand what type of kidney stone is being studied.

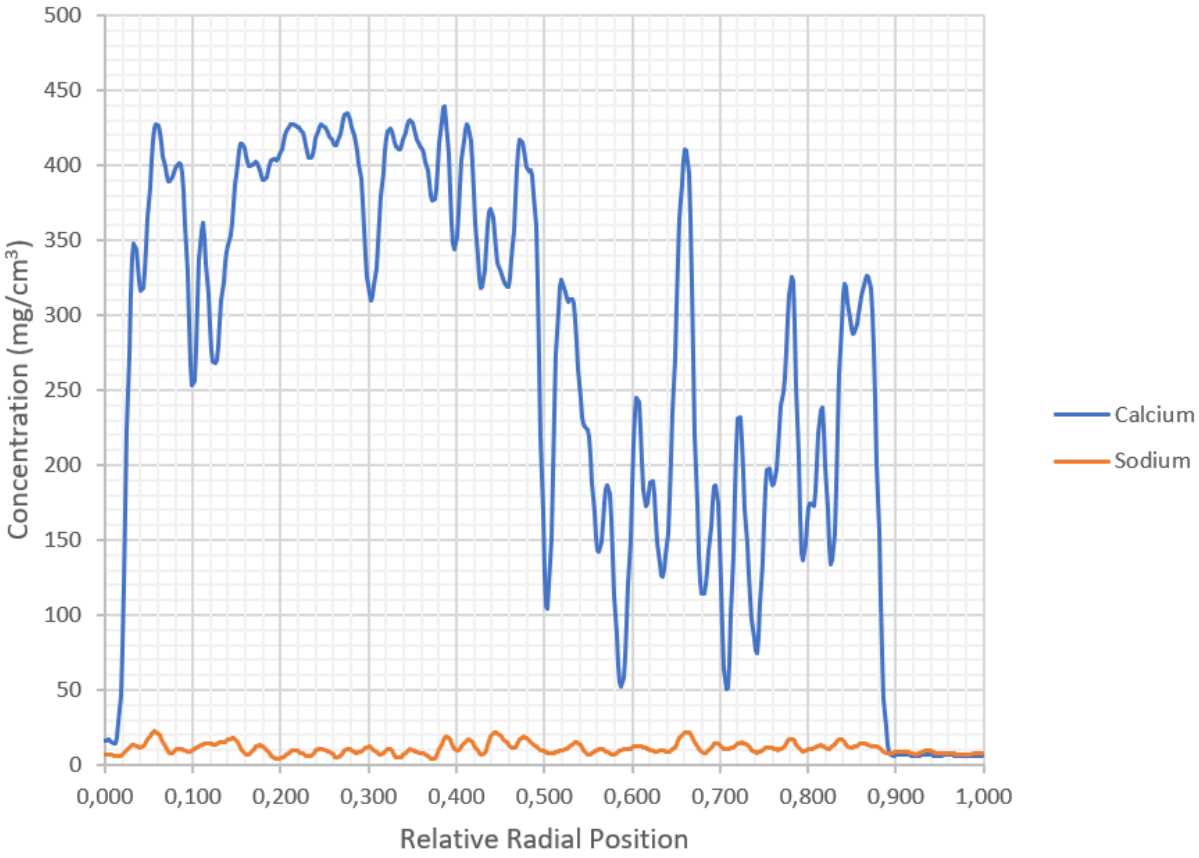

Figure 4.2. Trend of the concentration of calcium and of the concentration of sodium as a function of the radial position.

As mentioned, from the SEM-EDX analysis it has been possible to know the predominant compounds that form the stone by considering oxygen and carbon concentrations: more precisely, the ratio between the two concentrations is the slope of the straight line and it indicates the main compounds present in the stone, as shown in Figure 4.3.

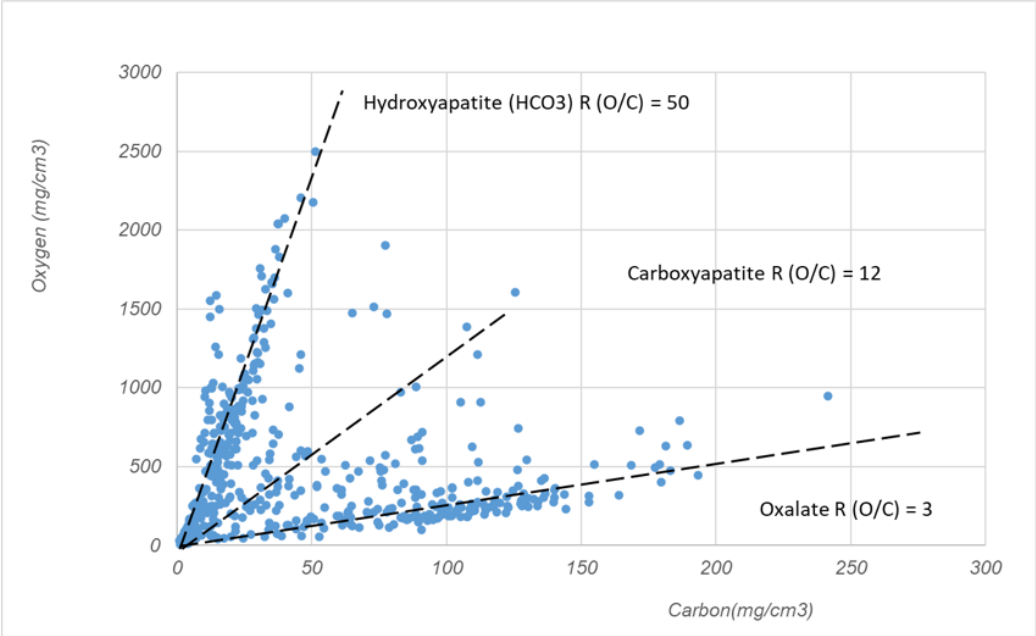

Figure 4.3. Predominant compounds in the examined stone.

As people eat, sleep, and work periodically over twenty-four hours, the variations in urine composition and supersaturation track the consequences of this behaviour. Urinary excretion of water and all major electrolytes exhibit circadian oscillations, and this kind of periodicity has been well documented during the years and greatly studied, as the great majority of physiological processes run with this rhythm.

The circadian rhythm marks the rate of urine formation by the kidney and it has been well demonstrated that the maximum excretion takes place during the activity phase (Firsov and Bonny, 2010). Furthermore, circadian fluctuations in the crystallization of urinary stones suggest that there may be a variability over twenty-four hours in the lithogenic risk (Robert *et al.*, 1994).

On the other side, relating this to what observed in the micrography in Figure 4.1, it is possible to conclude that the Liesegang ring-like layers equal to periodic waves of precipitation and peaks of urinary concentration. As a result, they reflect the biologic cycle of the renal system.

In this sense, it is possible to deduce that local supersaturation is a phenomenon that repeat itself over and over daily, and this allows to consider a circadian cycle for the lithogenic parameters in the urine and to detect the abnormal values.

There were noticeable variations in the excretion of the different urine constituents with time, but these were most evident for calcium.

By applying these conclusions to the presence of calcium in the stone, it is possible to consider each mean peak in Figure 4.2 as a period of time of twenty-four hours and, consequently, the distance between adjacent peaks as a day. In the case of calcium, twenty-one peaks and, therefore, twenty-one days, were considered.

Thus, it is possible to obtain the graph in figure 4.4, which characterizes the trend of the concentration of calcium as a function of time. Analogously, it is possible to build the graph that shows the mass variation of the kidney stone, always respect to the calcium, as a function of time (in days), as shown in Figure 4.5.

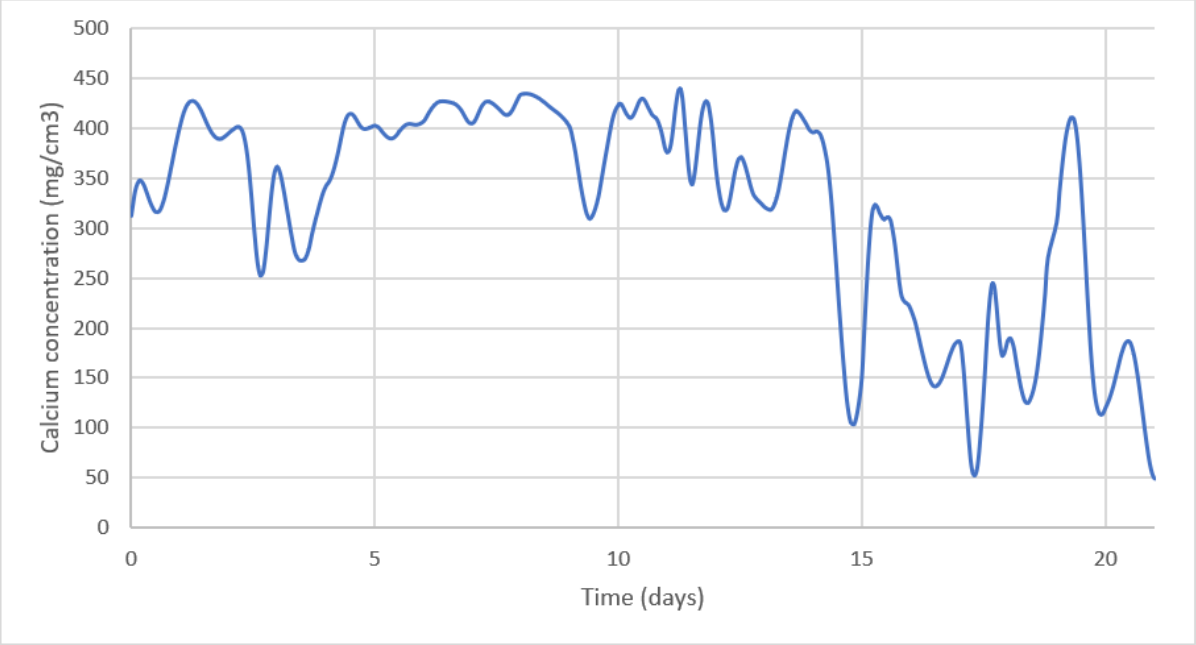

Figure 4.4. Calcium concentration (mg/cm3) as a function of time (days).

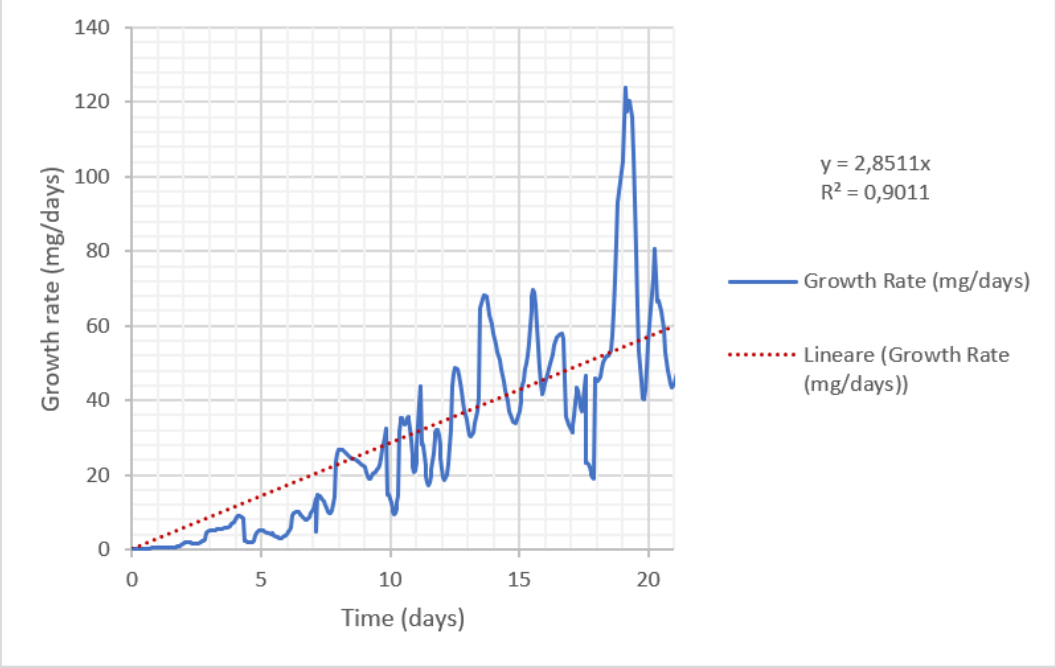

Figure 4.5. Mass variation of the urinary stone (mg/time) as a function of time (days).

From Figure 4.5, one thing appears noticeable: in the first days, it is possible to observe and oscillation of the values and then, the growth rate starts growing and increasing: this may be due to an advancement in the crystallization process.

It is important to highlight how, in reality, to build the graphs, it was necessary to consider how the measure with the SEM-EDX technique was carried out, which means by starting from the periphery up to the nucleus and not the other way around.

The observed trends allow to determine that the growth of the urinary stone and the adsorption of substances are two processes that happen simultaneously and in parallel during the day. This reflects the trend of the concentration with the radial position, as explained before.

In addition, a temporal growth sequence for the specific sample is estimated by means of the concentration profile obtained for calcium. For this, it has been used the circadian cycle studied by Ahlstrand *et al.* (1984) and Vahlensieck *et al.* (1982), whose investigations serve as a starting point to make a comparison between the calcium concentration profiles.

4.3.1 Urinary cycle

In an effort to check whether the precipitation waves achieved through SEM-EDX comply with the biochemical cycle of urine, the studies carried out by Ahlstrand *et al.* (1984) and Vahlensieck *et al.* (1982) have been taken as a basis. Both authors have studied the changes in the concentration of various elements in the urine over a total of 24 hours, showing considerable variation in the excretion of these elements, which are related to the different habits of a person during the day. For example, high calcium concentrations are observed at night when the patient is presumably asleep.

Focusing on calcium as an element of great importance in kidney stone formation, Figure 4.6 details the concentration data at different times of the day for a total of 24 hours.

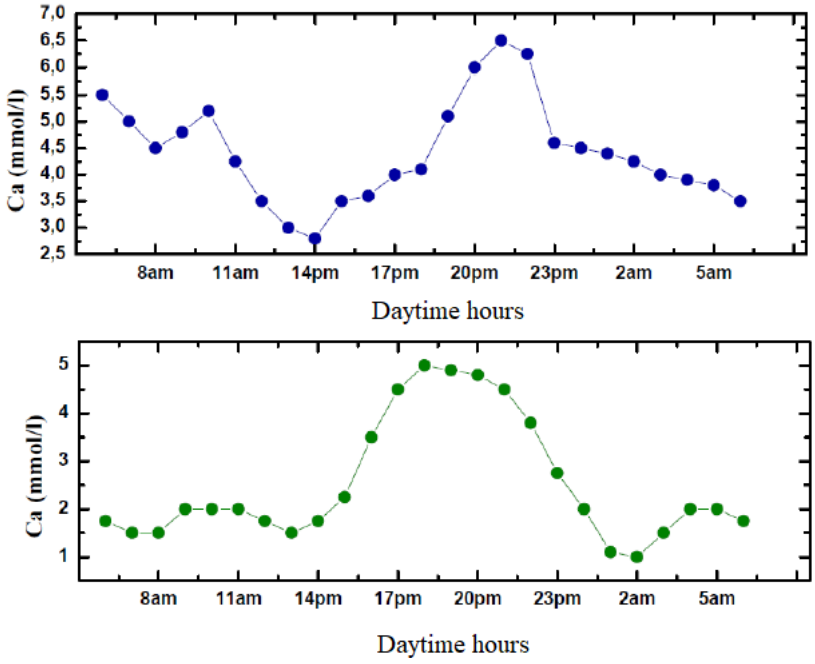

Figure 4.6. Circadian cycle for calcium in a lithiasic patient from 6 am to 6 am, as studied by Ahlstrand *et al.* (1984) above and Vahlensieck *et al.* (1982) below.

With a closed look at both graphs, between 20 pm and 23 pm there is a considerable peak in calcium concentration. This peak is maintained during a longer interval (from 17 pm to 23 pm) in the cycle studied by Vahlensieck *et al.* (1982). With respect to the rest of the hours that make up the day, around 6 am a slight peak in concentration is again observed in both, which is slightly observed at the beginning of the circadian cycle represented by Ahlstrand *et al.* (1984) and, more clearly, at the end of the cycle analysed by Vahlensieck *et al.* (1982).

In addition, in the interval between 8 am and 11 am, an increase in calcium concentration occurs (Figure 4.6, above), which is more smoothed in the cycle represented below in Figure 4.6.

Overall, it is possible to conclude that both cycles are relatively similar in terms of concentration profile trends.

In order to carry out a comparative study with the analysed sample, the biochemical cycle of the calcium in urine represented by Ahlstrand *et al*. (1984) has been taken as a reference, since it presents, as mentioned above, an additional peak in the concentration at around 10 am, which is not very clearly seen in the cycle proposed by Vahlensieck *et al*. (1982).

Observing the results obtained by SEM-EDX analysis, it has been proposed that each peak corresponds to the moment of maximum calcium concentration in the urine. This occurs once a day so that the time elapsed between the appearance of two successive peaks corresponds to 24h. In this way, a total growth time of the calculation of approximately 21 days has been estimated.

Figure 4.7 shows the circadian cycle obtained by Ahlstrand et al. (1984) for a total of 21 days.

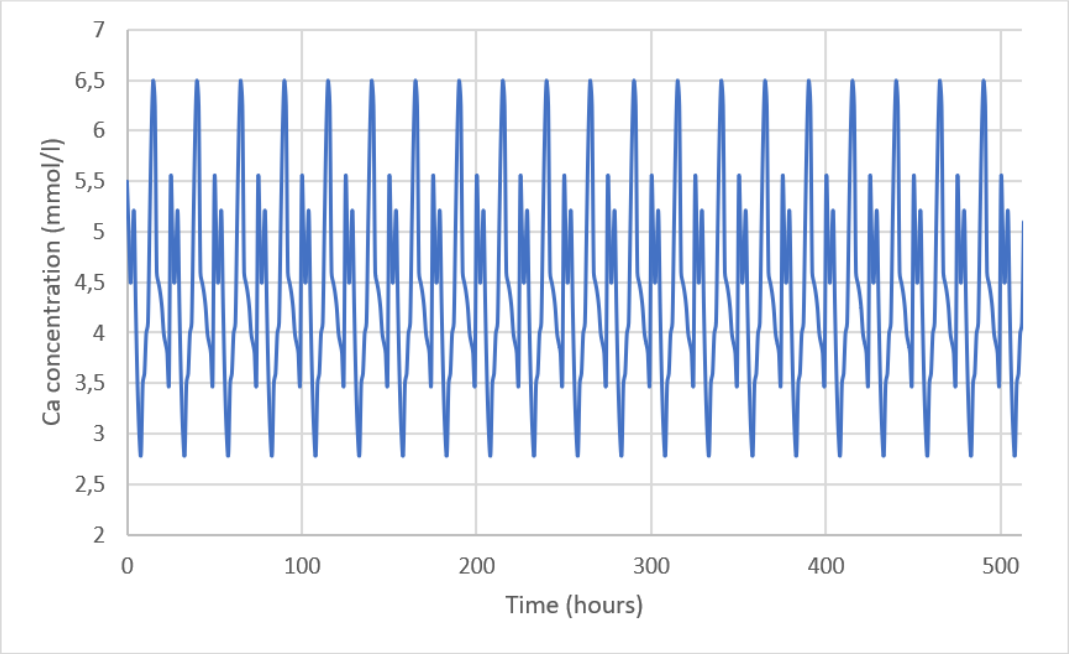

Figure 4.7. Calcium circadian cycle of 21 days according to data collected by Ahlstrand *et al.* (1984).

In order to see if the results obtained by the linear scanning technique can be related to the urine biochemical cycle observed in Figure 4.7, it is necessary to convert the data obtained in mg/cm^3 to mmol/l using the molecular weight of calcium. In addition, a numerical correlation has been established to relate the calcium concentration present in the kidney stone to the urinary calcium concentration at that time. Once the results have been obtained in the desired units, the data are smoothed, as they initially present excessive noise that hinders their analysis when superimposed on the cycle represented in Figure 4.7.

Furthermore, it should be noted that the data obtained by SEM-EDX are plotted against the radial position on the stone, with slight differences between the peak-to-peak distance. In other words, the peak-to-peak distance of concentrations is not constant throughout the whole kidney calculation. Therefore, in order to establish a time sequence according to the distance travelled, when scanning the kidney stone, the distance between various peaks was checked and, considering an average of 64 µm between peak and peak, it was concluded that every 16 steps (4 µm/step) the 24h established for each concentration peak were met.

In addition, it should be noted that the radial trajectory performed by SEM-EDX has been carried out from the periphery of the kidney stone to the core of the stone, so that it is necessary to invert the data so that day 1, corresponding to the beginning of stone formation, coincides with the data obtained for the central zone of the stone (core of the stone).

Figure 4.8 shows the precipitation pattern that has been matched to the urinary circadian cycle proposed by Ahlstrand *et al.* (1984) to test whether the hypothesis described above is valid. That is, if each calcium peak obtained by SEM-EDX corresponds to the maximum calcium concentration in urine.

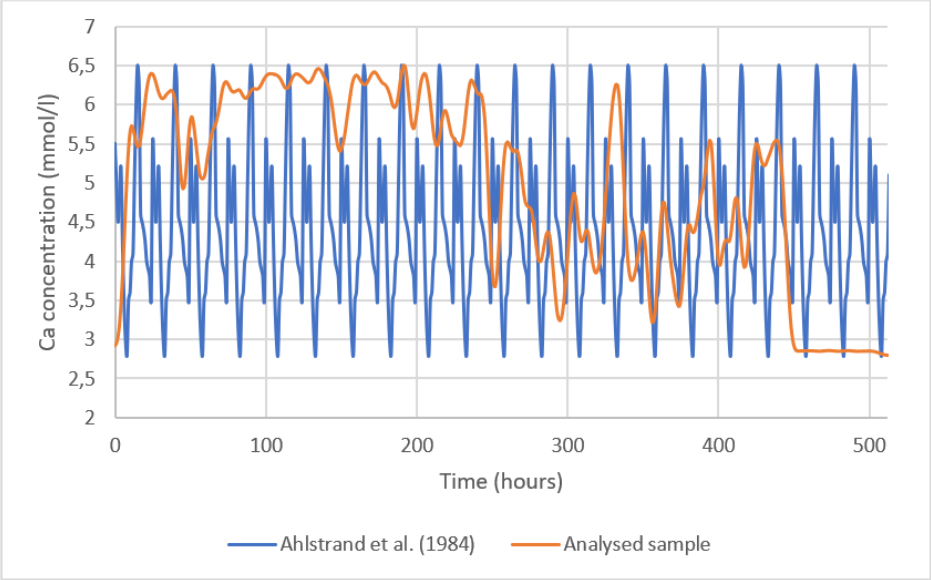

Figure 4.8. Comparison between the circadian cycles of calcium in 21 days.

In Figure 4.8 it is possible to recognize the peaks of concentration that coincide with the ones represented by Ahlstrand et al. (1984). Moreover, there are also peaks that show a slight temporal displacement, but it is conceivable to conclude that they are almost coincident with the circadian cycle studied from the bibliography.

A closer look at the graph shows that the concentration profile for the sample also coincides in several peaks at lower concentrations. Therefore, taking into account the peaks at high and low concentrations, as well as the peaks with a slight time shift, it is concluded that both circadian cycles coincide in 90.47 %. While, without taking into account those peaks with the slight time shift, a coincidence of 76.2 % is obtained. This confirms that the concentration profiles obtained using the innovative technique proposed in this study can be related to the biochemical urine cycle in patients suffering from renal lithiasis.

For what concerns the time range between 16 and 21 days, a sudden decrease of the calcium is observed, and it may correspond to the area where there may be a hole in the calculation produced at the time of the preparation of the stone for its analysis.

As a conclusion, Tables 4.8 – 4.9 and Tables 4.10 – 4.11 give the values obtained for the circadian cycle of calcium obtained by Ahlstrand *et al.* (1984) and for the chosen sample, respectively. In both, values at time 0 have been included, which correspond to the moments prior to the formation of the calculation.

Table 4.8. Concentrations of calcium (mmol/l) for a total of 21 days (Ahlstrand *et al.*, 1984).

	Days										
	0	1	2	3	4	5	6	7	8	9	10
Concentration of calcium (mmol/l) by Ahlstrand et al. (1984)	5,5	6,00	5,10	4,10	4,00	3,60	3,50	2,80	3,00	3,50	4,25
	5,0	6,50	6,00	5,10	4,10	4,00	3,60	3,50	2,80	3,00	3,50
	4,5	6,25	6,50	6,00	5,10	4,10	4,00	3,60	3,50	2,80	3,00
	4,8	4,60	6,25	6,50	6,00	5,10	4,10	4,00	3,60	3,50	2,80
	5,2	4,50	4,60	6,25	6,50	6,00	5,10	4,10	4,00	3,60	3,50
	4,3	4,40	4,50	4,60	6,25	6,50	6,00	5,10	4,10	4,00	3,60
	3,5	4,25	4,40	4,50	4,60	6,25	6,50	6,00	5,10	4,10	4,00
	3,0	4,00	4,25	4,40	4,50	4,60	6,25	6,50	6,00	5,10	4,10
	2,8	3,90	4,00	4,25	4,40	4,50	4,60	6,25	6,50	6,00	5,10
	3,5	3,80	3,90	4,00	4,25	4,40	4,50	4,60	6,25	6,50	6,00
	3,6	3,50	3,80	3,90	4,00	4,25	4,40	4,50	4,60	6,25	6,50
	4,0	5,50	3,50	3,80	3,90	4,00	4,25	4,40	4,50	4,60	6,25
	4,1	5,00	5,50	3,50	3,80	3,90	4,00	4,25	4,40	4,50	4,60
	5,1	4,50	5,00	5,50	3,50	3,80	3,90	4,00	4,25	4,40	4,50
		4,80	4,50	5,00	5,50	3,50	3,80	3,90	4,00	4,25	4,40
		5,20	4,80	4,50	5,00	5,50	3,50	3,80	3,90	4,00	4,25
		4,25	5,20	4,80	4,50	5,00	5,50	3,50	3,80	3,90	4,00
		3,50	4,25	5,20	4,80	4,50	5,00	5,50	3,50	3,80	3,90
		3,00	3,50	4,25	5,20	4,80	4,50	5,00	5,50	3,50	3,80
		2,80	3,00	3,50	4,25	5,20	4,80	4,50	5,00	5,50	3,50
		3,50	2,80	3,00	3,50	4,25	5,20	4,80	4,50	5,00	5,50
		3,60	3,50	2,80	3,00	3,50	4,25	5,20	4,80	4,50	5,00
		4,00	3,60	3,50	2,80	3,00	3,50	4,25	5,20	4,80	4,50
		4,10	4,00	3,60	3,50	2,80	3,00	3,50	4,25	5,20	4,80

Table 4.9. Concentrations of calcium (mmol/l) for a total of 21 days (Ahlstrand *et al.*, 1984), continuation.

	Days										
	11	12	13	14	15	16	17	18	19	20	21
Concentration of calcium (mmol/l) by Ahlstrand et al. (1984)	5,20	4,80	4,50	5,00	5,50	4,00	4,25	4,40	4,50	4,60	6,25
	4,25	5,20	4,80	4,50	5,00	3,90	4,00	4,25	4,40	4,50	4,60
	3,50	4,25	5,20	4,80	4,50	3,80	3,90	4,00	4,25	4,40	4,50
	3,00	3,50	4,25	5,20	4,80	3,50	3,80	3,90	4,00	4,25	4,40
	2,80	3,00	3,50	4,25	5,20	5,50	3,50	3,80	3,90	4,00	4,25
	3,50	2,80	3,00	3,50	4,25	5,00	5,50	3,50	3,80	3,90	4,00
	3,60	3,50	2,80	3,00	3,50	4,50	5,00	5,50	3,50	3,80	3,90
	4,00	3,60	3,50	2,80	3,00	4,80	4,50	5,00	5,50	3,50	3,80
	4,10	4,00	3,60	3,50	2,80	5,20	4,80	4,50	5,00	5,50	3,50
	5,10	4,10	4,00	3,60	3,50	4,25	5,20	4,80	4,50	5,00	5,50
	6,00	5,10	4,10	4,00	3,60	3,50	4,25	5,20	4,80	4,50	5,00
	6,50	6,00	5,10	4,10	4,00	3,00	3,50	4,25	5,20	4,80	4,50
	6,25	6,50	6,00	5,10	4,10	2,80	3,00	3,50	4,25	5,20	4,80
	4,60	6,25	6,50	6,00	5,10	3,50	2,80	3,00	3,50	4,25	5,20
	4,50	4,60	6,25	6,50	6,00	3,60	3,50	2,80	3,00	3,50	4,25
	4,40	4,50	4,60	6,25	6,50	4,00	3,60	3,50	2,80	3,00	3,50
	4,25	4,40	4,50	4,60	6,25	4,10	4,00	3,60	3,50	2,80	3,00
	4,00	4,25	4,40	4,50	4,60	5,10	4,10	4,00	3,60	3,50	2,80
	3,90	4,00	4,25	4,40	4,50	6,00	5,10	4,10	4,00	3,60	3,50
	3,80	3,90	4,00	4,25	4,40	6,50	6,00	5,10	4,10	4,00	3,60
	3,50	3,80	3,90	4,00	4,25	6,25	6,50	6,00	5,10	4,10	4,00
	5,50	3,50	3,80	3,90	4,20	4,60	6,25	6,50	6,00	5,10	4,00
	5,00	5,50	3,50	3,80	4,15	4,50	4,60	6,25	6,50	6,00	4,00
	4,50	5,00	5,50	3,50	4,10	4,40	4,50	4,60	6,25	6,50	4,00

Table 4.10. Concentrations of calcium (mmol/l) in the sample, for a total of 21 days.

	Days										
	0	1	2	3	4	5	6	7	8	9	10
Concentration of calcium in the sample (mmol/l)	2,8	2,85	2,85	4,50	4,36	5,29	3,51	4,27	4,51	4,06	4,65
	2,8	2,85	2,85	4,85	4,10	5,51	3,62	4,14	4,28	3,81	4,68
	2,8	2,85	2,85	5,14	3,95	5,54	3,74	4,00	4,10	3,59	4,70
	2,8	2,85	2,85	5,35	3,93	5,44	3,88	3,89	3,97	3,40	4,71
	2,9	2,86	2,85	5,48	4,03	5,29	4,04	3,81	3,90	3,28	4,75
	2,9	2,86	2,85	5,54	4,24	5,12	4,24	3,76	3,85	3,24	4,86
	2,9	2,86	2,86	5,55	4,48	4,97	4,45	3,76	3,87	3,26	5,02
	2,9	2,86	2,86	5,52	4,69	4,89	4,63	3,83	3,94	3,35	5,18
	2,9	2,86	2,86	5,49	4,81	4,81	4,75	3,99	4,05	3,53	5,30
	2,9	2,85	2,86	5,44	4,79	4,69	4,74	4,27	4,19	3,75	5,39
	2,9	2,85	2,86	5,38	4,66	4,56	4,58	4,66	4,33	3,98	5,42
	2,9	2,85	2,86	5,33	4,49	4,46	4,32	5,09	4,40	4,18	5,41
	2,9	2,85	2,86	5,28	4,33	4,38	3,98	5,52	4,38	4,33	5,40
	2,8	2,85	2,85	5,23	4,26	4,37	3,64	5,87	4,32	4,37	5,42
		2,85	2,85	5,22	4,26	4,41	3,37	6,13	4,27	4,35	5,46
		2,85	2,85	5,25	4,27	4,46	3,23	6,25	4,25	4,27	5,51
		2,86	2,85	5,31	4,24	4,46	3,22	6,26	4,34	4,15	5,52
		2,86	2,87	5,40	4,16	4,36	3,34	6,19	4,51	4,05	5,49
		2,86	2,92	5,49	4,04	4,17	3,56	6,06	4,70	4,00	5,35
		2,86	3,01	5,50	3,95	3,94	3,82	5,87	4,84	4,00	5,10
		2,86	3,17	5,44	3,99	3,70	4,08	5,63	4,87	4,09	4,78
		2,86	3,42	5,27	4,20	3,51	4,27	5,37	4,77	4,22	4,42
		2,85	3,75	4,99	4,54	3,43	4,37	5,08	4,59	4,39	4,07
		2,85	4,12	4,67	4,93	3,44	4,36	4,78	4,34	4,54	3,81

Table 4.11. Concentrations of calcium (mmol/l) in the sample, for a total of 21 days.

	Days										
	11	12	13	14	15	16	17	18	19	20	21
Concentration of calcium in the sample (mmol/l)	3,68	5,49	6,37	6,23	6,13	6,39	6,37	6,14	5,15	6,17	5,70
	3,69	5,51	6,30	6,26	6,00	6,34	6,38	6,18	5,07	6,15	5,73
	3,88	5,53	6,19	6,27	5,86	6,31	6,39	6,19	5,05	6,13	5,65
	4,23	5,56	6,05	6,29	5,72	6,29	6,39	6,18	5,07	6,10	5,43
	4,64	5,58	5,90	6,31	5,59	6,28	6,40	6,17	5,13	6,08	5,10
	5,09	5,62	5,77	6,34	5,50	6,29	6,40	6,16	5,27	6,08	4,67
	5,51	5,70	5,70	6,38	5,43	6,31	6,40	6,17	5,44	6,11	4,22
	5,83	5,79	5,73	6,41	5,41	6,33	6,38	6,19	5,62	6,16	3,79
	6,01	5,87	5,85	6,42	5,45	6,35	6,36	6,22	5,77	6,22	3,44
	6,11	5,92	6,04	6,41	5,54	6,37	6,34	6,26	5,85	6,29	3,19
	6,14	5,91	6,23	6,39	5,67	6,38	6,30	6,29	5,80	6,36	3,03
	6,13	5,83	6,41	6,35	5,82	6,39	6,26	6,29	5,63	6,39	2,95
	6,15	5,71	6,50	6,31	5,97	6,40	6,23	6,25	5,39	6,40	2,92
	6,21	5,58	6,50	6,28	6,09	6,38	6,21	6,17	5,13	6,37	2,95
	6,26	5,49	6,41	6,26	6,18	6,36	6,20	6,06	4,96	6,30	3,03
	6,30	5,48	6,29	6,26	6,25	6,32	6,20	5,95	4,93	6,19	3,19
	6,31	5,54	6,15	6,28	6,30	6,27	6,21	5,85	5,05	6,04	3,44
	6,26	5,66	6,03	6,30	6,34	6,23	6,20	5,77	5,29	5,87	3,79
	6,14	5,84	5,98	6,33	6,38	6,21	6,18	5,72	5,58	5,70	4,22
	5,98	6,03	5,97	6,36	6,42	6,21	6,14	5,68	5,84	5,56	4,67
	5,80	6,18	6,00	6,38	6,45	6,24	6,10	5,62	6,02	5,48	3,50
	5,64	6,30	6,07	6,36	6,46	6,28	6,08	5,51	6,13	5,46	
	5,54	6,38	6,14	6,32	6,46	6,32	6,09	5,40	6,18	5,52	
	5,49	6,40	6,19	6,25	6,43	6,35	6,11	5,28	6,18	5,61	

4.4 Evaluation of the supersaturation level

The supersaturation of urine with respect to lithiatic compounds, like magnesium phosphates, calcium phosphates and calcium oxalates, is fundamental and has an important role in the development of renal stones or, more in general, in the formation of solid precipitates in the urinary tract and in the kidney, so in the risk of stone formation (Finleyson B., 1982).

Since the next step is the evaluation of the supersaturation level in urine, it is important to know that the analytic calculation of the supersaturation of urine with respect to stone formation leads to some kind of incomplete determination, since the urine composition is assumed without considering all the nearly 76 species present in it and, also, considering some fixed actual urinary pH. This is due the violation of the electroneutrality condition, which is the law that affirms that every solution of an electrolyte or a mixture of electrolytes must be electroneutral (the negative charges balance the positive charges).

Additionally, ion pairings that do not consider all species present in a significant concentration leads to an overestimation of the simple ion concentrations, such as Ca^{2+} and $C_2O_4^{2-}$; therefore, an overestimation of the supersaturation.

The achievement of a correct thermodynamic value of the supersaturation is crucial in the kinetic studies of renal calculi and in the progress of growth rate investigations.

Nevertheless, since from the SEM-EDX analysis it was possible to know and discover the main compounds forming the studied bladder stone, the attention will be focused on the predominant compounds in the calculus and, thus, the urine supersaturation will be evaluated with respect to them.

4.4.1 Urine composition

Urine is a complicated aqueous system containing numerous inorganic and organic ions and complexes and undissociated organic compounds. Inorganic components, namely sodium, potassium, ammonium, magnesium, calcium, phosphates, chlorides, sulfates, carbonates and several organic components, predominately oxalates, citrates, uric acid and its salts, are present in urine in various forms—simple ions and charged and uncharged ion pairs (Söhnel *et al.*, 2018).

As explained before, calcium is present as ions, ion pairs and complexes, which means that only a part of all the total calcium precipitates as a substance composed by ionic species. The same applies to phosphorus, as at a physiological urine pH value, it is present in two different forms: $H_2PO_4^-$ and HPO_4^{2-}.

To solve the problem, also due to the fact that human urine composition varies between people and throughout the day, a representative average urine composition will be considered, as shown in Table 4.4.1.

In addition, the total concentration of calcium and phosphate will be expressed as Ca^{2+} and HPO_4^{2-} (Söhnel y Grases, 2010) and an average and constant urine pH equal to 6 will be considered, so the concentrations of the two ions will be considered as constant too.

Table 4.4.1. Average urine composition.

Compound	Charge	Concentration (mmol/L)
Na^+	1	75
K^+	1	30
Mg^{2+}	2	1.8
Ca^{2+}	2	2.5
HPO_4^{2-}	-2	5
Cl^-	-1	100
NH_4^+	1	7
Oxalate	2	0.165
Citrate	3	2.01

Other useful physical characteristics of urine can be listed in Table 4.4.2 (Anatomy and Physiology, 2016). It can be convenient to know that urine density is often referred to as specific gravity, as it is a measure of the quantity of solutes per unit volume of a solution. Also, an average volume of 1 L will be considered in further calculations.

In these conditions, the ionic strength, calculated with the Equation (3.10), will have the following value:

$$I = 0.135 \ {}^{mol}/_{L}$$

Table 4.4.2. Physical characteristics of urine.

Physical property	Minimum value	Maximum value
Volume (mL/24 hours)	750	2000
pH	4.5	8
Density	1.003	1.032

It has been proved (Söhnel and Grases, 2011) that the solubility constant does not vary significantly in the range between 25 °C (standard condition of temperature) and 37 °C (average body temperature and urine temperature), so in order to evaluate the level of supersaturation it is possible to consider the solubility constant at 25 °C.

In order to evaluate the supersaturation level in a simple way, the growth rate will be considered. Furthermore, it is assumed that all the calcium in the urine will participate at the formation of the stone.

By taking into account the concentration of calcium in the stone and the average concentration of calcium ions in the urine, it is possible to evaluate the variation of the supersaturation level, as shown in Figure 4.9.

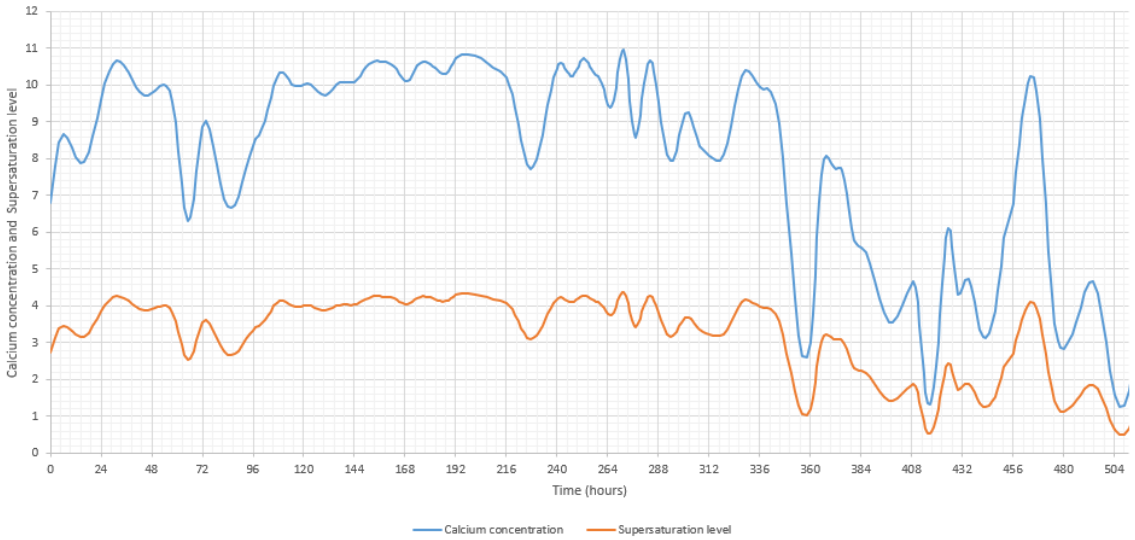

Figure 4.9. Supersaturation level and concentration of calcium over time.

From Figure 4.9, it is clearly noticeable how the supersaturation level over time follows the path of the concentration of calcium. The supersaturation level over time varies in the following range:

$$\Gamma = 0.502 - \ 4.384$$

This equals a correspondent range of calcium concentration in urine:

$$C_{Ca^{2+}} = 1.256 \ - \ 10.960 \ {}^{mmol}/_{L}$$

4.4.2 Comparison with the supersaturation level obtainable from Ahlstrand *et al.* (1984).

Along the lines of what already done with the evaluation of a circadian cycle, to determine the range of oversaturation in the literature data, the urine calcium concentration was divided by the average calcium concentration in healthy urine (which signifies its respective value shown in Table 4.4.2). In this case, the supersaturation range obtained in the sample corresponding to the literature is:

$$\Gamma = 1.120 - \ 2.620$$

Figure 4.10 shows the supersaturation for the sample analysed by Ahlstrand *et al.* (1984) for 24h.

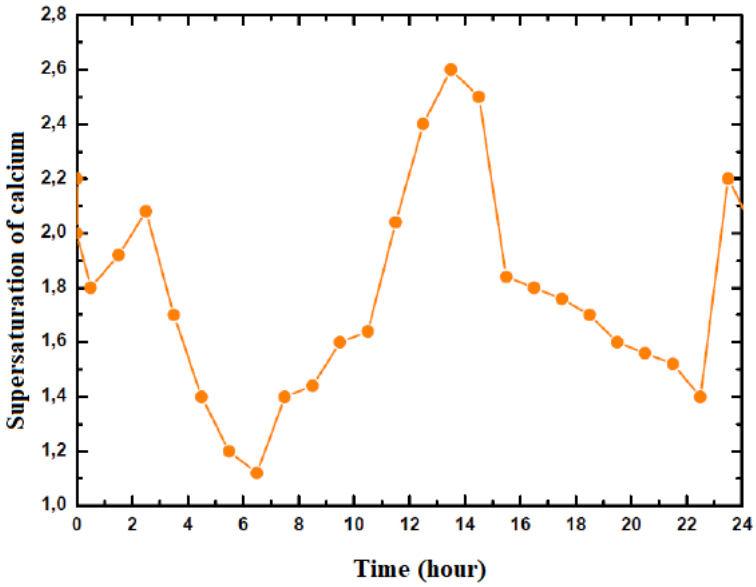

Figure 4.10. Supersaturation corresponding to the literature sample (adapted from Ahlstrand *et al.*, 1984).

Ultimately, it is possible to represent the supersaturation of calcium for the chosen sample during a total time of 21 days (Figure 4.11), comparing it with the literature data.

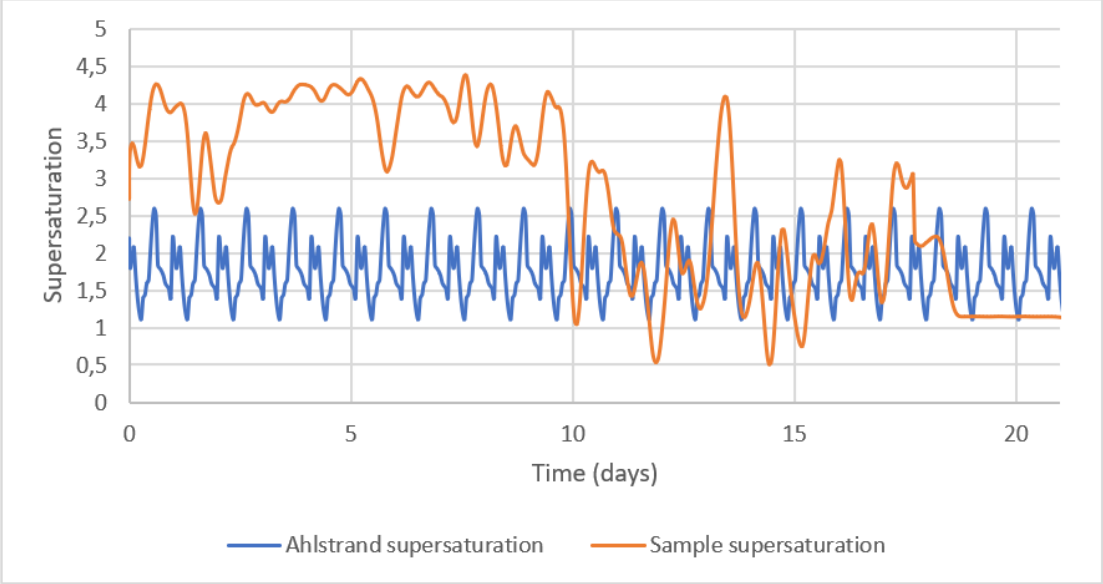

Figure 4.11. Supersaturation of calcium during a temporal sequency of 21 days for the chosen sample compared with the supersaturation obtained from literature data during the same period of time.

Despite the considerable differences in values, due to the dissimilarities in calcium concentrations considered, the general trend in supersaturation can be compared with that derived from the bibliography considered for this study.

5. Results discussion

5.1 Preliminary considerations

In light of the results achieved, the simple kinetic model hypothesized in chapter 3 will be corrected and applied to what obtained.

The adjusted kinetic model will be as simple as before: it has been said that the growth of the renal calculus (which means the width of the ring-like layers) is considered as independent from the position or the dimension of the stone and this means that the kinetics is controlled by the mass transfer from the bulk solution (the urine) to the external layer of the particle, and this will be described thanks to the mass transfer coefficient k_L. The interfacial effects and the electrochemical effects will be not considered; hence, these assumptions will lead to the following kinetic model (Equation 5.1.):

$$v_g = k_L(\sigma_i - 1)S_i^* \tag{5.1}$$

Where S_i^* is the supersaturation of the considered crystalline phase.

5.2 Explication of the kinetic approximation of the growth of the renal calculus "in vivo"

Even though there ae a lot of discussions on the chemical and crystalline transformations that happen in the interior part of the lithiatic mass, from a kinetic point of view it is possible to quantitatively consider that renal calculi only have an exclusively superficial growth.

This equals to affirm that the growth of the particle is controlled by mass transfer from the bulk of the liquid phase (urine) to the film phase between the external layer of the solid and the liquid bulk. Accordingly, being $J_{i,el}$ the superficial flux of the predominant crystalline species i, and A_p the external surface of the particle, the growth rate of the lithiatic mass vg will have the following form (Equation 5.2):

$$v_g = \frac{dm_i}{dt} = A_p J_{i,el} \tag{5.2}$$

Clearly, if various species i are quantitatively co-precipitating, it is possible to consider the sum of all the different growth rates (5.3):

$$v_g = \sum_{i=1}^{N} A_p J_{i,el} \tag{5.3}$$

By considering a first approximation, Fick's law can be considered as valid. This equals to consider as negligible the superficial effects that certain substances can introduce through interfacial tension, or the electrochemical effects derived from ionic flow associated with crystallization, or others related to pressure or the presence of impurities or the crystallinity of the solid phase (Equation 5.4).

$$J_i = k_L \Delta C_i \tag{5.4}$$

In the solid-liquid interphase, dissolution happens when the substance finds itself at the concentration of saturation S_i^*, hence the driving gradient can be written as following (Equation 5.5):

$$\Delta C_i = (\sigma_i - 1) S_i^* \tag{5.5}$$

This leads to consider the mass (Equation 5.6) for a majoritarian elemental compound j:

$$m_i = \rho_p \cdot V_p \cdot x_i \tag{5.6}$$

There is a proportionality between the concentration in the solid phase and the solubility of the precipitating crystalline species and, considering x_i as the mass fraction of the component, this can be expressed as in the Equation (5.7):

$$\alpha_i = {}^{x_i}/_{S_i^*} \tag{5.7}$$

This leads to the following Equation (5.8) for the growth rate:

$$v_g = \frac{dm_i}{dt} = \frac{d(\rho_p \cdot V_p \cdot x_i)}{dt} = A_p \cdot k_L \cdot (\sigma_i - 1) \cdot S_i^* \tag{5.8}$$

This is valid considering the pseudo-stationary state for the particle. By considering the following equations (from Equation 5.9 to Equation 5.11), it will be possible to conclude that the growth rate of the renal calculus dimension (which means the radius of the particle r_p) is constant over time if the supersaturation level and the hydrodynamic conditions in the particle environment are maintained.

$$\rho_p \cdot \frac{d(V_p)}{dt} = \left(\frac{A_p \cdot k_L}{\alpha_i}\right) \cdot (\sigma_i - 1) \tag{5.9}$$

$$\rho_p \cdot 4\pi {r_p}^2 \frac{d(r_p)}{dt} = \left({4\pi {r_p}^2 \cdot k_L}/{\alpha_i}\right) \cdot (\sigma_i - 1) \tag{5.10}$$

$$\frac{d(r_p)}{dt} = \left(\frac{k_L}{\alpha_i \cdot \rho_p}\right) \cdot (\sigma_i - 1) \tag{5.11}$$

The discussion will lead to the results for the different crystalline species.

The Nernst – Planck kinetic model for the flux of ions through the external surface of the stone can be applied too, but with the introduction of an apparent factor, function of the mass transfer coefficient and of the Nernst – Planck potential. Indeed, Equation 5.11 can be seen as a connection between the first approximation of the flux as Fick – type and the Nernst – Planck – type flux.

6. Conclusions, remarks, future perspectives

This master's degree project aimed at a deep investigation of the growth stage of a bladder calculus formation process. In order to achieve the objectives of this study, it has been essential the prior acquisition of an extensive knowledge on the whole development of the lithiatic process; hence, a deep literature research has been done.

The most important accomplished and reached goals in the evaluation of a kinetic model are the following:

- The linear scanning of the SEM-EDX has proven to be a powerful tool for morpho-compositional analysis of urinary stones. Although the raw data from these analyses have a high level of noise, this can be removed with the application of an SMA filter to clearly show trends and growth cycles.
- The concentration of selected substances doesn't vary consistently in the solid phase, and the same happens with the respective solubility;
- Local supersaturation is a phenomenon that repeat itself over and over daily, and this allows to consider a circadian cycle for the lithogenic parameters in the urine and to detect the abnormal values;
- Small fluctuations in stone composition must be related to the function of the renal system, as these have been found to be a reflection of the biochemical cycling of the urine. Consequently, a cycle that changes the lithogenic parameters of the urine (concentration of ions promoting to inhibiting crystallisation) causes the growth of these bands;
- The fluctuations observed by SEM-EDX also provide information for the estimation of the time sequence of kidney stone growth, as each concentration peak can correspond to a day of stone formation;
- The growth of the stone initially oscillate but, then, starts growing and increasing: this may be due to an advancement in the crystallization process;
- The stone growth is a kinetically controlled phenomenon;
- The growth rate of the crystal depends on supersaturation but, most of all, on the chemical potential, which is the real driving force behind the whole process of growth;
- The Liesegang ring-like layers equal to periodic waves of precipitation and peaks of urinary concentration and, as a result, they reflect the biologic cycle of the renal system;
- The growth rate of the renal calculus dimension (which means the radius of the particle r_p) is constant over time if the supersaturation level and the hydrodynamic conditions in the particle environment are maintained;
- The growth rate can be related with a description related to the Nernst – Planck equation describing the flux of ions through a membrane and considering a corrective factor;
- The calcium concentration profile follows a very similar trend to that observed in the circadian cycle reported in the literature. Therefore, it is considered that the

concentration patterns obtained by SEM-EDX on the stone are related to the biochemical cycle of the urine;

- Using this new tool, unlike the other analysis techniques used so far, it would be possible to establish a chronological sequence of stone growth and, with this information, relate its appearance to the different intrinsic and extrinsic factors of renal lithiasis and the patient's lifestyle.

This work is, actually, only a step in the whole research and investigation on the lithiatic process: in fact, the formation of renal calculi is still object of study, as it is partially unknown.

As far as the growth process (in the strict sense) of kidney stone is concerned, a new frontier of knowledge in this area can be the study of the influence of surface effects and pressure variations on the flow of ions through the surface of the stone. This type of approach would thus allow to broaden the knowledge on the nature of the causes of the formation and, consequently, hopefully help prevent or treat this really common disease.

List of symbols

Δa	variation of activity
ΔC	variation of concentration (mol/l)
ΔG	variation of Gibbs free energy (J/mol)
a	activity (-)
A	constant (0.509 $mol^{-1/2}kg^{1/2}$)
a_{eq}	activity at equilibrium
A_p	external surface of the particle (mm^2)
a_s	activity in the solution
C	concentration (mol/l)
C_{eq}	concentration at equilibrium (mol/l)
C_s	concentration in the solution (mol/l)
$Ct_j(r)$	counts of the j-element
D_i	molecular diffusion coefficient (m^2/s)
F	Faraday constant (96485.332 $Cmol^{-1}$)
g	growth rate (g/s)
I	ionic strength (mol/l)
J_i	molar flowrate (mol/s)
k	constant (g/s)
K_1	value of the equilibrium constant for temperature T1 (-)
K_2	value of the equilibrium constant for temperature T2 (-)
k_b	Boltzmann constant ($1.381 \cdot 10^{-23}$ JK^{-1})
k_j	conversion factor
k_L	transport coefficient (mm/s)
K_{sp}	solubility constant (-)
m_j	mass of the j-element (kg)
m_T	total mass of the stone (kg)
n	stoichiometric coefficient (-)
N_A	Avogadro number ($6.022 \cdot 10^{23}$ mol^{-1})
q	elementary charge (-)
R	ideal gas constant (8.314 J/molK)
r	radius (m)
r_p	radius of the particle (m)
S*	supersaturation (-)

T_1	reference temperature (298.15 K)
T_2	process temperature (310,15 K)
V_m	molar volume (mm^3/mol)
V_p	volume of the particle (mm^3)
X_j	ratio between m_j and m_T (-)
$x_j(r)$	volume of the j-element (mg/mm^3)
z_i	charge (-)
ΔH_r°	enthalpy of reaction when both reactants and products are in their standard state and at 25 °C (298.15 K)
ρ_p	density of the particle (kg/m^3)

Greek symbols

α_i	proportionality factor (-)
γ	coefficient of activity (l/mol)
Γ	supersaturation (-)
ε_0	vacuum permittivity (8.854 (C^2/Nm^2)
ε_r	relative permittivity (-)
$\Delta\mu$	variation of chemical potential (J/mol^{-1})
μ^0	standard chemical potential (J/mol^{-1})
μ_{eq}	chemical potential at equilibrium (J/mol^{-1})
μ_s	chemical potential in the solution (J/mol^{-1})
σ	relative supersaturation (-)
φ_i	electric potential (V)

Bibliography

Ahlstrand, C., Larsson, L., & Tiselius, H. G., 1984, Variations in urine composition during the day in patients with calcium oxalate stone disease. *Journal of Urology*, **131(1)**: 77–81.

Androulakis Ioannis P., 2014, A chemical engineer's perspective on health and disease. *Computers and Chemical Engineering* **71**: 665–671.

Boistelle R., 1985, Concepts de la cristallisation en solution., *Actual Nephrol*, **15**:159–202.

Borghi L, Schianchi T, Meschi T, et al., 2002, Comparison of two diets for the prevention of recurrent stones in idiopathic hypercalciuria. *N Engl J Med*., **346(2)**:77-84.

BOYCE WH, GARVEY FK and NORFLEET CM, 1954, Ion-binding properties of electrophoretically homogeneous mucoproteins of urine in normal subjects and in patients with renal calculus disease. *J Uro* **72**:1019—1031.

BOYCE WH, KING JS and FIELDEN ML, 1962, Total nondialyzable solids (TNDS) in human urine: XIII. Immunological detection of a component peculiar to renal calculous matrix and to urine of calculous parients. *J C/in Invest* **41**:1180—1189.

Brener ZZ, Winchester JF, Salman H, et al., 2011, Nephrolithiasis: evaluation and management. *Southern Medical Journal*, **104(2)**: 133-9.

Buchman TG., 2010, Novel representation of physiologic states during critical illness and recovery. *Crit Care*. **14**:127.

Cloutier J., Villa L., Traxer O. and Daudon M., 2015, Kidney stone analysis: "Give me your stone, I will tell you who you are!", *World J Urol* **33**: 157 – 169.

Coe FL., 1978, Hyperuricosuric calcium oxalate nephrolithiasis. *Kidney Int.*, **13(5)**:418-426.

Corbo J. and Wang J., 2019, Kidney and Ureteral Stone. *Emerg Med Clin North Am.*, **37**(4), 637-648.

Curhan GC and Taylor EN., 2008, 24-h uric acid excretion and the risk of kidney stones. *Kidney Int*., **73(4)**:489-496.

Curhan GC, Willett WC, Rimm EB and Stampfer MJ., 1993, A prospective study of dietary calcium and other nutrients and the risk of symptomatic kidney stones. *N Engl J Med*., **328**:833-838.

Curhan GC, Willett WC, Rimm EB and Stampfer MJ., 1993, A prospective study of dietary calcium and other nutrients and the risk of symptomatic kidney stones. *N Engl J Med.*, **328**:833-838.

Daudon M. and Jungers P., 2012, Stone composition and morphology: a window on etiology. In: Talati JJ, Tiselius HG, Albala DM, Ye Z (eds) *Urolithiasis: basic science and clinical practice*. Springer, London, pp 113–140.

Daudon M., 2014, Litogénesis, *EMC - Urología*, **46(1)**: 1–14.

Daudon M., Dessombz A., Frochot V., Letavernier E., Haymann J.P., Jungers P. and Bazin D., 2016, Comprehensive morpho-constitutional etiological diagnosis and therapeutic strategy of nephrolithiasis, *C. R. Chimie,* **19**: 1470-1491

Debschitz Uv, Kahn F and Debschitz Tv. Fritz Kahn, 2009, *Man machine* [Maschine mensch].Wien/New York: Springer; 2009.

Dr. Cesar A Restrepo V, 2007, Anatomia y Fisiologia. *Anatomia y Fisiologia*, pp 790–795.

Enciclopedia medica italiana, 1988, USES, Edizioni Scientifiche Firenze, II Edizione, 12: 1324 – 1352.

Finlayson B, 1982, Pathologic mineralization, nucleation, growth, and retention. In: *Nancollas GH (ed) Biological Mineralization and demineralization*. Report of the Dahlem workshop on biological mineralization and demineralization. Springer, Berlin, 18–23 Oct 1981, p 271.

Finlayson Birdwell, 1978, Physicochemical aspects of urolithiasis, *Kidney International*, Vol. 13, pp. 344—360.

Firsov Dmitri and Bonny Oliver, 2010, Circadian regulation of renal function, *Kidney International*, **78**: 640 – 645.

Foster G., Stocks C. and Borofsky MS., 2009, *Emergency Department Visits and Hospital Admissions for Kidney Stone Disease*, Statistical Brief #139. Healthcare Cost and Utilization Project (HCUP) Statistical Briefs [Internet]. Rockville (MD): Agency for Healthcare Research and Quality (US); 2006–2012.

Garcia-Garcia, S., Millán-Rodríguez, F., Rousaud-Barón, F., Montañés-Bermúdez, R., Angerri-Feu, O., Sánchez-Martín, F., Villavicencio-Mavrich, H., & Oliver-Samper, A., 2011, Why and how we must analyse urinary calculi. *Actas Urologicas Espanolas*, **35(6)**:354–362.

Goldfarb DS, Fischer ME, Keich Y. and Goldberg J., 2005, A twin study of genetic and dietary influences on nephrolithiasis: a report from the Vietnam Era Twin (VET) Registry. *Kidney Int.,* **67(3)**: 1053-1061.

Gómez Ayala, A. E., 2015, *Litiasis Renal*. **22(2)**: 4.

Grases F, Conte A and Costa-Bauzá A., 2001, Tipos de cálculos renales. Relación con la bioquímica urinaria. *Arch Esp de Urol*; **54**(9): 861-871.

Grases F, Costa-Bauzá A, Ramis M, Montesinos V, Conte A., 2002, Simple classification of renal calculi closely related to their micromorphology and etiology. *Clin Chim Acta*. **322(1-2)**: 29-36.

Grossmann IE and Morari M., 1983, Operability, resiliency and flexibility – process design objecives for a changing world. In: *Proceedings second international conference foundation of computer aided process design*.

Grover PK, Marshall VR, Ryall RL., 2003, Dissolved urate salts out calcium oxalate in undiluted human urine in vitro: Implications for calcium oxalate stone genesis. *Chem Biol.* **10**:271–278.

Holmes RP and Assimos DG., 2004, The impact of dietary oxalate on kidney stone formation. *Urol Res.*, **32(5)**:311-316.

Johnson CM, Wilson DM, O'Fallon WM, Malek RS and Kurland LT., 1979, *Renal stone epidemiology: a 25-year study in Rochester, Minnesota*. Kidney Int. **16(5)**:624-631.

Jones WHS., 1924, *The Doctor's Oath: an essay in the history of medicine*. London: Oxford University Press.

Kavanaugh J.P., 2006, Supersaturation and renal precipitation: the key to stone formation? *Urol Res* **34**: 81 – 85.

Killeen, A. A., 2017, Riñones. *Abbott Diagnostics*.

Lieske JC, de la Vega LS Peña and Slezak JM., 2006, Renal stone epidemiology in Rochester, Minnesota: an update. *Kidney Int*., **69(4)**: 760-764.

M. ROBERT., ROUX. F. BOURELLY, A.M. BOULARAN, J. GUITER and L. MONNIER, 1994, Circadian variations in the risk of urinary calcium oxalate stone formation, *British Journal of Urology*, **74**: 294-297.

María, P., García, G., Isabel, M., Yanes, L., García, V., 2019, Nefrología, S., Candelaria, H. U. N. S., Candelaria, N. P. D. H. U. N. S., & Litogénesis, I. Litiasis Renal.

MARSHALL RW, COCHRAN M, ROBERTSON WG, HODGKINSON A and NORDIN BEC, 1972, The relation between the concentration of calcium salts in the urine and renal stone composition in patients with calcium-containing renal stones. *Clin Sci*, **43**:433—441.

Mente A, Honey RJ, McLaughlin JR, Bull SB and Logan AG., 2007, Ethnic differences in relative risk of idiopathic calcium nephrolithiasis in North America. *J Urol.*, **178(5)**:1992-1997. discussion 1997.

Mijangos F., Celaya M.A., Gainza F.J. and Eunate Arana A.I., 2020, SEM-EDX linear scanning: a new tool for morpho-compositional analysis of growth bands in urinary stones. *J Biol Inorg Chem*, June 2020.

Moran M.E., 2014*, Urolithiasis: A Comprehensive History*, Springer, 2nd Edition, New York, **1**, 1-3.

Moran ME., 2010, *Andreas Vesalius and seminal errors. De Historia Urologiae Europaeae*, **17**, 102–15.

National Kidney and Urologic Diseases Information Clearinghouse (NKUDIC), 2009, *National Institutes of Health*.

OpenStax, 2016, *Anatomy & Physiology*. OpenStax, CNX. Feb 26, 2016.

P. W. Atkins, 1999, *Química física*, Ediciones Omega S.A., Sexta Edición.

Prein EL., 1963, Crystallographic analysis of urinary calculi: a 23-year survey study. *J Urol*., **89**, 917–924.

Rao Nagaraja P., Preminger Glenn M. and Kavanagh John P., 2011, *Urinary Tract Stone Disease*, Springer, London, **3**: 36 – 49.

ROBERTSON WG, MARSHALL RW and PEACOCK M. KNOWLES F, 1976, The Saturation of urine in recurrent, idiopathic calcium stone-formers, in *Urolithiasis Research*, edited by FLEISCH H, ROBERTSON WG, SMITH LH, VAHLENSIECK W, New York, Plenum Press, pp. 335—338.

ROBERTSON WG, PEACOCK M and N0RDIN BEC, 1968, Activity products in stone-forming and non-stone forming urine., *Clin Sci,* **34**:579—594.

Rodríguez Fernández, L. M., 2013, Morfología y función renal. *Pediatría Integral*.

S. Klein, 2018, *Il racconto della Chimica e della Terra*, Zanichelli editore.

Scales CD Jr, Curtis LH, Norris RD, et al., 2007, Changing gender prevalence of stone disease. *J Urol.*; **177(3)**: 979-982.

Scales CD, Smith AC, Hanley JM, et al., 2012, *Urologic Diseases in America Project: Prevalence of kidney stones in the United States*, Eur Urol.; **62**:160–5.

Söhnel O. and Grases F., 2011, Supersaturation of body fluids, plasma and urine, with respect to biological hydroxyapatite. *Urol Res* **39**:429–436.

Söhnel O., Loučka T. & Grases F., 2018, Speciation and supersaturation of urine. *Monatsh Chem* **149**: 333–339.

Stoller ML and Bolton DM., 1995, Urinary stone disease. In: Tanagho EA, McAninch JW, eds. *Smith's general urology*, 14th ed. Los Altos, California, Appleton and Lange, 298.

Taylor EN and Curhan GC., Body size and 24-hour urine composition., 2006, *Am J Kidney Dis*., **48(6)**:905-915.

Vahlensieck, E. W., Bach, D., & Hesse, A., 1982, Circadian rhythm of lithogenic substances in the urine. *Urological Research*, **10(4)**: 195–203.

Winslow Teresa, 2020, Kidney Cancer, CDC. Centros Para El Control y La Prevención de Enfermedades, from https://www.cdc.gov/spanish/cancer/kidney/index.htm

Zauner R and Jones AG., 2000, Determination of nucleation, growth, agglomeration and disruption kinetics from experimental precipitation data: the calcium oxalate system. *Chem Eng Sci.*, **55**:4219–4232.

Zhou Danna, 2015, Applications of Chemical Equilibrium Diagram Software HYDRA/MEDUSA in Teaching College Chemistry. *University Chemistry*, Vol. 30, Issue **4**: 21 – 25.

Ringraziamenti

In primis, grazie ai miei genitori, per essermi stati accanto, avermi sostenuto sempre e averci creduto, anche e soprattutto al posto mio. Grazie ad Artù, a cui questa tesi è dedicata, per avermi dato in soli due anni tutto l'amore, la fedeltà, le carezze di cui non sapevo neanche di avere bisogno e avermi ricordato che il tempo non limita l'affetto in alcun modo, anche se ne avrei voluto di più.

Grazie a Patricia, senza la quale questo lavoro di tesi non sarebbe stato possibile; grazie a Natalia, per avermi aiutata lungo tutto il mio (mancato) Erasmus ed esser diventata mia amica, senza neanche avermi mai vista. Spero di poter recuperare il prima possibile.

Grazie a Sarah, Simo e Fra, per aver reso quel che era partito come un Erasmus normale ed è terminato con una quarantena e un ritorno commosso, un'esperienza che sicuramente mi porterò dentro per sempre. Non avrei potuto desiderare compagne di "viaggio" migliori.

Grazie ai miei amici, quelli veri, quelli che ci sono da sempre e quelli che ci sono da meno, per esser rimasti sempre, anche quando la prima a volersene andare ero io; quindi, citando Susanna Casciani, "grazie a chi non è rimasto indifferente, a chi non si è nascosto di fronte al dolore, a chi mi abbraccia senza difendersi. Grazie a chi non mi ha mai detto: «Cosa vuoi che sia», a chi ha provato a capire come mai certe volte mi manca il respiro. A chi si ricorda che vado pazza per il vino rosso, a chi se ne frega di quello che ho e che non ho e si prende cura di quello che sono. A chi mi ha insegnato ad ammettere di avere paura, a chi mi ha insegnato a chiedere aiuto, ché non è vero che siamo sempre in grado di farcela da soli: certe volte abbiamo bisogno di farcela insieme a qualcuno. Grazie a chi mi ha costretto a fare i conti con la mia tristezza, a chi mi ha ricordato quanto sia importante piangere, a chi mi ha regalato un libro, a chi ha pensato a me ascoltando una canzone e poi mi ha detto: «Devi assolutamente sentirla». Grazie a chi si fa in quattro per condividere la bellezza". Ad ognuno di voi, grazie, dal profondo del cuore.

Infine, più che un grazie, uno scusa: a me stessa, per guardarmi spesso ma senza vedermi davvero.